A Graphical Method for Estimation of Barometric Efficiency from Continuous Data—Concepts and Application to a Site in the Piedmont, Air Force Plant 6, Marietta, Georgia

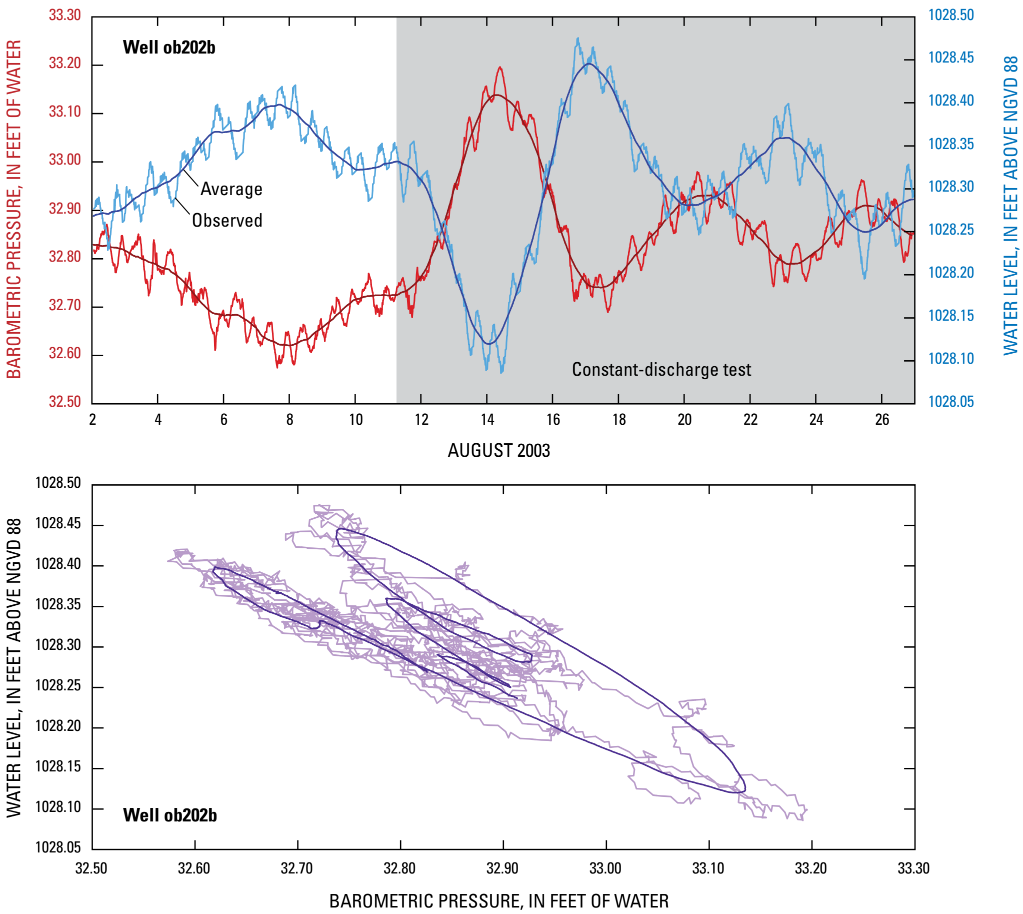

Scientific Investigation Report 2007-5111

Prepared in cooperation with the
U.S. Air Force Aeronautical Systems Center, Marietta, Georgia

U.S. Department of the Interior
U.S. Geological Survey

A Graphical Method for Estimation of Barometric Efficiency from Continuous Data—Concepts and Application to a Site in the Piedmont, Air Force Plant 6, Marietta, Georgia

By Gerard J. Gonthier

Prepared in cooperation with the
U.S. Air Force Aeronautical Systems Center, Marietta, Georgia

Scientific Investigation Report 2007-5111

U.S. Department of the Interior
U.S. Geological Survey

U.S. Department of the Interior
DIRK KEMPTHORNE, Secretary

U.S. Geological Survey
Mark D. Myers, Director

U.S. Geological Survey, Reston, Virginia: 2007

For product and ordering information:
World Wide Web: *http://www.usgs.gov/pubprod*
Telephone: 1-888-ASK-USGS

For more information on the USGS--the Federal source for science about the Earth, its natural and living resources, natural hazards, and the environment:
World Wide Web: *http://www.usgs.gov*
Telephone: 1-888-ASK-USGS

Suggested citation:
Gonthier, G.J., 2007, A Graphical Method for Estimation of Barometric Efficiency from Continuous Data—Concepts and Application to a Site in the Piedmont, Air Force Plant 6, Marietta, Georgia: U.S. Geological Survey Scientific Investigations Report 2007-5111, 29 p., Web-only publication available at *http://pubs.usgs.gov/sir/2007/5111/*.

Contents

Figures

Tables

Datums

Vertical coordinate information is referenced to the North American Vertical Datum of 1988 (NAVD 88).

Horizontal coordinate information is referenced to the North American Datum of 1983 (NAD 83).

A Graphical Method for Estimation of Barometric Efficiency from Continuous Data—Concepts and Application to a Site in the Piedmont, Air Force Plant 6, Marietta, Georgia

By Gerard J. Gonthier

Abstract

A graphical method that uses continuous water-level and barometric-pressure data was developed to estimate barometric efficiency. A plot of nearly continuous water level (on the y-axis), as a function of nearly continuous barometric pressure (on the x-axis), will plot as a line curved into a series of connected elliptical loops. Each loop represents a barometric-pressure fluctuation. The negative of the slope of the major axis of an elliptical loop will be the ratio of water-level change to barometric-pressure change, which is the sum of the barometric efficiency plus the error.

The negative of the slope of the preferred orientation of many elliptical loops is an estimate of the barometric efficiency. The slope of the preferred orientation of many elliptical loops is approximately the median of the slopes of the major axes of the elliptical loops. If water-level change that is not caused by barometric-pressure change does not correlate with barometric-pressure change, the probability that the error will be greater than zero will be the same as the probability that it will be less than zero. As a result, the negative of the median of the slopes for many loops will be close to the barometric efficiency.

The graphical method provided a rapid assessment of whether a well was affected by barometric-pressure change and also provided a rapid estimate of barometric efficiency. The graphical method was used to assess which wells at Air Force Plant 6, Marietta, Georgia, had water levels affected by barometric-pressure changes during a 2003 constant-discharge aquifer test. The graphical method was also used to estimate barometric efficiency. Barometric-efficiency estimates from the graphical method were compared to those of four other methods: average of ratios, median of ratios, Clark, and slope. The two methods (the graphical and median-of-ratios methods) that used the median values of water-level change divided by barometric-pressure change appeared to be most resistant to error caused by barometric-pressure-independent water-level change. The graphical method was particularly resistant to large amounts of barometric-pressure-independent water-level change, having an average and standard deviation of error for control wells that was less than one-quarter that of the other four methods.

When using the graphical method, it is advisable that more than one person select the slope or that the same person fits the same data several times to minimize the effect of subjectivity. Also, a long study period should be used (at least 60 days) to ensure that loops affected by large amounts of barometric-pressure-independent water-level change do not significantly contribute to error in the barometric-efficiency estimate.

Introduction

Barometric efficiency is the water-level change caused by a barometric-pressure change divided by that barometric-pressure change (Clark, 1967). In confined aquifer settings, an increase in barometric pressure usually will cause a decrease in water level in an open well by an amount governed by the barometric efficiency (Todd, 1959; Ferris and others, 1962; Freeze and Cherry, 1979; Kruseman and de Ridder, 1991; Landmeyer, 1996; Rasmussen and Crawford, 1997; and Batu, 1998). Aquifer-test methods depend on accurate measurements of pumpage-induced ground-water-level fluctuations for determining values of hydraulic properties. The barometric efficiency is used, as a correction factor, to remove barometric effects on water levels in wells during an aquifer test (Kruseman and de Ridder, 1991), and also can be used to help determine the degree of confinement within an aquifer to which the well is opened (Landmeyer, 1996), estimate the storage coefficient in a confined aquifer (Jacob, 1940), and determine bulk elastic properties of the aquifer (Domenico, 1983; Rojstaczer and Agnew, 1989; Batu, 1998). Determination of barometric efficiency is challenging because it is difficult to distinguish the component of water-level change within a well caused by barometric-pressure change from the total water-level change within a well.

Water-level and barometric-pressure data were collected at Air Force Plant 6, Marietta, Georgia, during 2003 as part of ground-water characterization efforts (fig. 1). An aquifer test was conducted during August and September 2003. Beginning about 2 days after the start of the aquifer test, barometric pressure rose and fell during a period of about 5 days by a maximum pressure of 10 millimeters of mercury (equivalent to about 0.43 foot of water). Several wells responded with a water-level decline followed by a water-level increase, respectively. The barometric effects on water level had to be removed to better interpret the aquifer-test data. A graphical method was developed to assess the wells that had water levels affected by barometric-pressure changes during the aquifer test and to estimate the barometric efficiency.

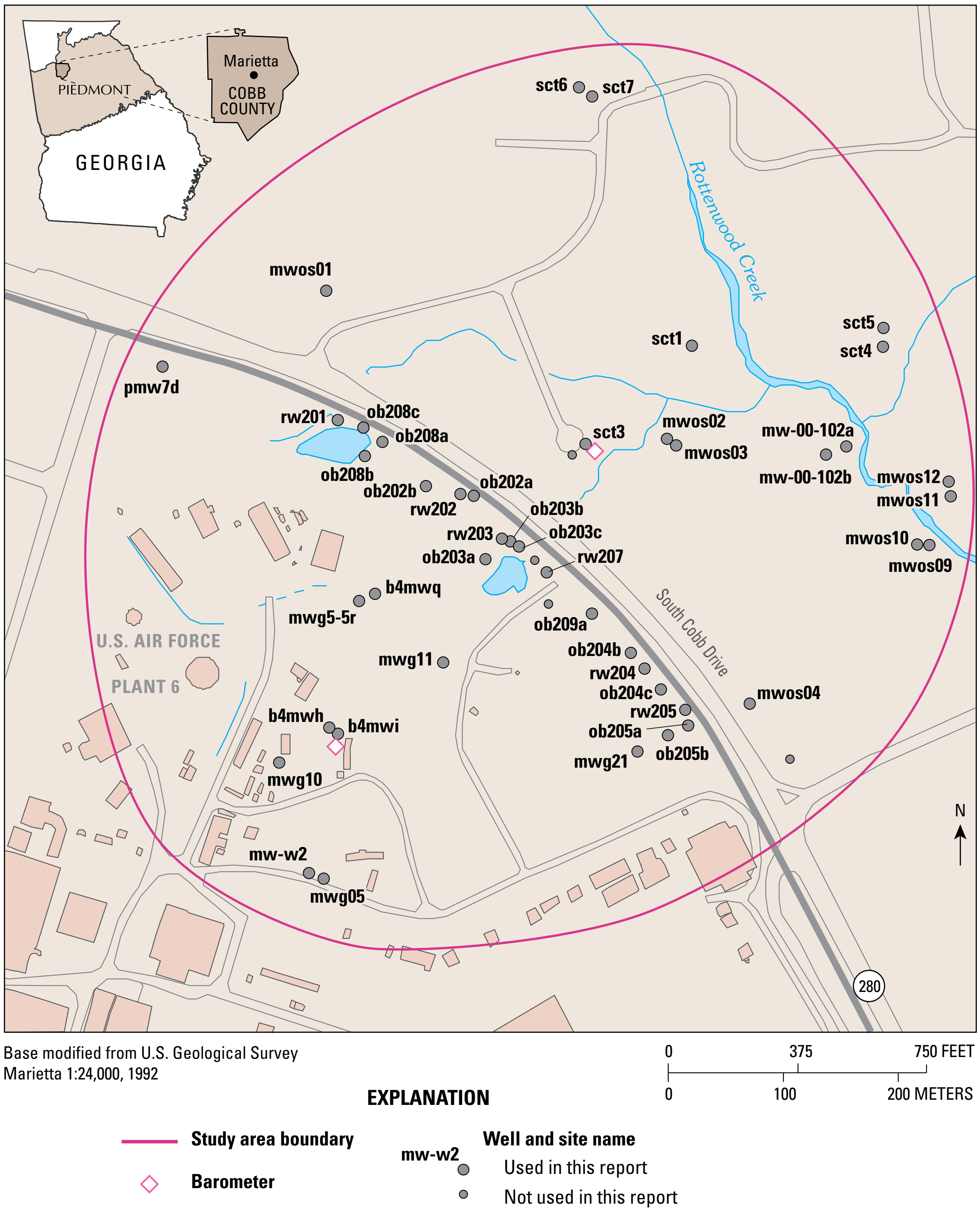

Figure 1. Monitoring wells in the study area, U.S. Air Force Plant 6, Marietta, Georgia, 2003.

Purpose and Scope

This report introduces a graphical method that estimates barometric efficiency rapidly and accurately, using continuous water-level and barometric-pressure data. Extensive background discussion and comparison with other methods are provided to support the graphical method. This report also provides general information on how to make the best estimates of barometric efficiency, emphasizing, but not limited to, continuous data. General discussion includes sources of error in estimating barometric efficiency, how to reduce some of that error prior to estimation, and how various methods reduce the effect of the remaining error during estimation. Water-level change that is not caused by barometric-pressure change, referred to in this report as "barometric-pressure-independent water-level change," is identified as the source of error in estimates of barometric efficiency. This report describes two simple techniques to remove some of the barometric-pressure-independent water-level change prior to using the data to estimate barometric efficiency. A technique for optimally selecting time intervals from barometric-pressure data also is presented. This report includes the theory behind the graphical method and examples of barometric-efficiency estimates using data from 45 wells at Air Force Plant 6, Marietta, Georgia. The graphical method is objectively compared to the four other methods in two separate ways.

Some examples described within this report are for wells opened to fractured, highly heterogeneous rock under various degrees of weathering (Air Force Plant 6, Marietta, Georgia; fig. 1). Because some of the examples in this report are for a fractured-rock setting and because of the possibility of well-bore storage and skin effects, estimates of barometric efficiency are considered for individual wells and not the "aquifer." Hereinafter, "water-level change" refers to water-level change within a well that is open to the atmosphere.

Acknowledgments

The U.S. Geological Survey conducted the research for this report at Air Force Plant 6, Marietta, Georgia. The U.S. Air Force Aeronautical Systems Center funded all research activities for this report. The following hydrologists from the U.S. Geological Survey contributed colleague reviews: Gregory S. Cherry, Earl A. Greene, James E. Landmeyer, Dorothy F. Payne, and Lynn J. Torak. Todd C. Rasmussen, Associate Professor of Hydrology at the University of Georgia, also contributed to the author's understanding of barometric effects on water levels in very shallow wells.

Barometric-Efficiency Concepts

Basic concepts that are used in this report to estimate barometric efficiency are discussed below. In this section, how barometric-pressure changes affect water levels in wells is briefly discussed, barometric efficiency is defined, the type of water-level change that adversely affects the estimation of barometric efficiency is identified, and how a method reduces the adverse effect of some water-level change during estimation is explained.

The term *study period* is defined in this report as the entire length of time that water-level and barometric-pressure data are available to determine barometric efficiency (one measurement, every 15 minutes for about 60 days). The term *time interval* describes a shorter length of time (from 6 hours to 2 days), which is usually the length of time used to determine values of water-level change (ΔW) and barometric-pressure change (ΔB). The term *time increment* refers to a shorter length of time between measurements taken by continuous-recorder equipment (for example, 15 minutes) and when ΔW and ΔB are sometimes determined.

Barometric-Pressure Effects on Water Levels

As early as 1663, Blaise Pascal (Pascal, 1973; Gossard and Hooke, 1975; Crawford, 1994) found barometric-pressure changes affected water levels in some wells. Todd (1959), Freeze and Cherry (1979), Batu (1998), and others provide a detailed description of how barometric-pressure change affects water levels in wells open to confined aquifers. An aquifer with a sturdy skeletal structure will keep some of the increase in barometric pressure at the surface from translating to water in the aquifer. Meanwhile, the full increase in barometric pressure will load onto the water level of a well open to the atmosphere. This results in an imbalance in pressure between water inside and outside of the well opening. The water level in the well changes to compensate for the imbalance by:

$$\Delta W_b = \frac{(\Delta P_{at} - \Delta P_{aq})}{\gamma_w}, \tag{1}$$

where

ΔW_b is the water-level change that is caused by barometric-pressure change, in units of length;

ΔP_{at} is the pressure change at the top of water in the well and at the land surface, in units of force per area;

ΔP_{aq} is the pressure change in the aquifer (water outside of the well screen) as a result of the pressure change at the land surface (ΔP_{at});

and

γ_w is the specific weight of the water in the well, in units of force per volume.

By convention set by literature (Clark, 1967; Batu, 1998), an increase in water level during a time interval is a positive change (greater than zero); but an increase in pressure during a time interval, is a negative change (less than zero).

Weeks (1979), Rasmussen and Crawford (1997), and Spane (1999) described the effect of barometric-pressure change on water level in wells open to unconfined aquifers.

Within the unconfined setting, there is a time lag between an increase in atmospheric pressure at land surface and its translation to the water table. The key factors causing the delay are the pneumatic diffusivity of air through the unsaturated zone and the thickness of the unsaturated zone. The result is that the water level in a well will respond to an instantaneous change in atmospheric pressure where the ΔP_{aq} in equation 1 is significantly less than ΔP_{at} at time zero. Through time, the increase in pressure at the surface migrates to the water table, ΔP_{aq} will increase to the value of ΔP_{at} in equation 1, and the water in the well will recover to its level prior to the pressure change. Barometric-pressure change will not affect a well that is directly connected to a surface-water feature (the effective thickness of the unsaturated zone is zero) or when the top of the well screen is above the water table.

Other factors that affect barometric efficiency of a well include well-skin and well-bore storage effects. A well with a clogged well screen or relatively impermeable material surrounding the well screen (well skin) will have a delayed response to barometric-pressure change (Rasmussen and Crawford, 1997; and Spane, 1999) and may cause the barometric efficiency (see definition below) to change with time. In this report, discussion of how methods estimate the barometric efficiency focuses on confined settings, and assumes that barometric efficiency does not change with time.

Barometric Efficiency

The definition of barometric efficiency equates to the following:

$$\alpha = \frac{\Delta W_b}{\Delta B}\ , \qquad (2)$$

where

ΔW_b is that part of the water-level change caused by a barometric-pressure change ΔB

and

α is the barometric efficiency.

The barometric-pressure change (ΔB) equates to $\Delta P_{at}/\gamma_w$, and is measured in units of length of water.

As with the previously mentioned pressure change, an increase in barometric pressure during a time interval is a negative change (Clark, 1967; Batu, 1998). The barometric efficiency is dimensionless and ranges from zero to one.

The water level, in time series, then can be corrected for barometric effects by:

$$W_{(t)corr} = W_{(t)uncorr} - \alpha\left(B_0 - B_{(t)}\right), \qquad (3)$$

where

$W_{(t)corr}$ is the water level, at time t, corrected for barometric pressure;

$W_{(t)uncorr}$ is the uncorrected water level, at time t ;

α is the barometric efficiency;

and

$(B_0 - B_{(t)})$ is the barometric pressure $B_{(t)}$, at time t, referenced to a barometric-pressure datum B_0.

Factors Influencing Water-Level Change

Measurable water-level change in a well (ΔW) is the water level in a well at time ($t+1$), minus the water level in a well at time (t):

$$\Delta W = W_{(t+1)} - W_{(t)}. \qquad (4)$$

Barometric-pressure change (ΔB) that causes the water-level change (ΔW_b) is measurable as the barometric pressure at time (t) minus the barometric pressure at time ($t+1$):

$$\Delta B = B_{(t)} - B_{(t+1)}\ . \qquad (5)$$

The order of time (t) and time ($t+1$) in equation 4 is inverted with respect to equation 5 in order to follow the convention that ΔB is negative for an increase in barometric pressure during a time interval. Throughout this report, plots of ΔW (on the y-axis) and ΔB (on the x-axis) for wells that are affected by barometric-pressure change have *positive* slopes whereas plots of W (on the y-axis) and B (on the x-axis) for the same data sets have *negative* slopes.

The measurable water-level change (ΔW) in a well is caused by one or more of several possible causes:

$$\Delta W = \Delta W_b + \Delta W_r + \Delta W_l + \Delta W_p + \Delta W_g + \Delta W_m + \Delta W_e + \Delta W_s + \Delta W_o, \qquad (6)$$

where

ΔW is the water-level change in a well during a time interval;

ΔW_b is the water-level change caused by barometric-pressure change;

ΔW_r is the water-level change caused by recharge;

ΔW_l is the water-level change caused by seasonal or long-term trends;

ΔW_p is the water-level change caused by local or regional pumping;

ΔW_g is the water-level change caused by earth tides;

ΔW_m is the water-level change caused by ocean tides;

ΔW_e is the water-level change caused by evapotranspiration;

ΔW_s is the water-level change caused by surface-water fluctuations;

and

ΔW_o is the water-level change caused by other influences, during a specific time interval.

Water-level change that is caused by recharge (ΔW_r) can be from rain events or snow melt. Examples of recharge used within this report are rain events. The response to a rain event is characterized by a sharp increase in water level, followed by a recession curve with the rate of water-level change decreasing with time after the rain event.

Seasonal or long-term trends (ΔW_l) involve water-level changes during lengths of time greater than barometric-pressure fluctuations. If one season is wetter than another, a long-term climate pattern will be reflected in water-level data during a study period. This long-term trend may be represented through time as a linear (constant change) or higher-order curved line.

Water-level change caused by pumping (ΔW_p) includes aquifer tests and other local pumping, or irrigation and other regional pumping. Regional pumping often occurs on a seasonal time scale, but the effects may be more pronounced during a shorter period of time. Study periods used to determine barometric efficiency and other correction factors should be during a time outside of an aquifer test (Halford, 2006).

Gravitational influences of the sun and moon along with movements of the moon and earth create changes in gravitational force on the earth (Rinehart, 1975). These forces cause earth tides. Earth tides are slight changes in the shape of the geoid that, in turn, lead to compression or tension within the earth's crust. For example, when the vertical component of the force of gravity is relatively high, the fractured-crystalline rock at Air Force Plant 6 usually is compressed, fractures constrict, storage is temporarily decreased, and the water in the fractures is squeezed to higher values of head. Conversely, when the force of gravity is relatively low, the fractured-crystalline rock is stretched, fractures dilate, storage is temporarily increased, and values of head decline. The result is the occurrence of sinusoidal fluctuations in water level (ΔW_g, two peaks and two troughs during about 25 hours) and a change in amplitudes, which cycles every 2 weeks (Marine, 1975; Domenico, 1983; and Galloway and Rojstaczer, 1988). Earth-tide effects are not to be confused with ocean-tide effects, which affect some wells that are close to the coast.

Ocean tides cause water-level change in wells (ΔW_m) by compression of a confined aquifer due to the increased weight of ocean water during high tide (Robinson and Bell, 1971; Batu, 1998). Under a confined aquifer setting, the ocean-tidal efficiency plus the barometric efficiency should, theoretically, equal one. Ocean tides cause water-level change in wells open to unconfined aquifers due to the head-gradient-induced flow of water into the unconfined aquifer.

Evapotranspiration from vegetation during daylight hours can act as local pumping in shallow aquifers. The water level in the well reaches a peak during sunrise and reaches a minimum just after sunset. There is a peak and trough each day with a wavelength of 1 day. Effects of evapotranspiration on ground-water level (ΔW_e) are greatest during the growing season and normally do not affect ground-water levels during winter when the temperature stays at or below freezing.

Wells that are in close proximity or have fractures directly connected to surface-water bodies may respond directly to surface-water fluctuations (ΔW_s). Surface-water bodies include ponds and streams. Wells near streams may exhibit water-level fluctuations that look like responses to rain events but are actually responding to a combination of rain events and stream-flood events.

Identifying Water-Level Change that Causes Error in Barometric-Efficiency Estimation

Water-level change that is caused by barometric-pressure change (ΔW_b) cannot be directly measured. Equation 6 can be simplified by grouping all of the water-level fluctuations that are independent of barometric-pressure change into one term (ΔW_i):

$$\Delta W = \Delta W_b + \Delta W_i \,. \tag{7}$$

Equation 7 separates the measurable water-level change in a well into two separate components based on their cause. While the term ΔW_b is the water-level change that is caused by barometric-pressure change (related to the "$\alpha \left(B_0 - B_{(t)}\right)$" in equation 3), the term ΔW_i is the water-level change that is not caused by barometric-pressure change (related to $W_{(t)corr}$ in equation 3). In this report, the terms W_i, W, and B are values relative to an implied reference datum.

From equations 2 and 7, it can be seen that the ratio of the total water-level change to the barometric-pressure change ($\Delta W/\Delta B$) is an estimate of barometric efficiency ($\hat{\alpha}$) and can be defined as:

$$\hat{\alpha} = \frac{(\Delta W_b + \Delta W_i)}{\Delta B} \,,$$

or (8)

$$\hat{\alpha} = \frac{\Delta W_b}{\Delta B} + \frac{\Delta W_i}{\Delta B} \,,$$

where

$\Delta W_b + \Delta W_i$ is the measurable water-level change (ΔW)

and

$\hat{\alpha}$ may or may not be close to the actual value of the barometric efficiency.

Rearranging equation 8 and substituting α for $\Delta W_b / \Delta B$ yields:

$$\hat{\alpha} - \alpha = \varepsilon_{sr} = \frac{\Delta W_i}{\Delta B} \,. \tag{9}$$

It can be seen that the error (ε_{sr}) in the estimate of barometric efficiency determined from a single ratio of water-level change to barometric-pressure change ($\Delta W/\Delta B$) is the ratio of barometric-pressure-independent water-level change to barometric-pressure change ($\Delta W_i / \Delta B$).

The key to an accurate estimation of barometric efficiency is to reduce the error-causing effect of barometric-pressure-independent water-level change (represented by ΔW_i) from the estimation (Clark, 1967; and Davis and Rasmussen, 1993). Some barometric-pressure-independent water-level change can be removed prior to estimating barometric efficiency because it can be identified and avoided or quantified and removed. Examples of avoidable ΔW_i include features that can be seen on hydrographs, such as spikes in water level associated with rain events or sudden decreases in water level caused by the start of pumping. Other forms of ΔW_i that can be removed from the data include long-term trends and daily fluctuations. Techniques for removing such barometric-pressure-independent water-level change are reviewed in the *Filtering Water-Level Change that Causes Error in the Estimation of the Barometric Efficiency* section of this report. After removing as much barometric-pressure-independent water-level change as possible, some barometric-pressure-independent water-level change will remain in the data.

Methods that estimate barometric efficiency do so in the presence of remaining barometric-pressure-independent water-level change. The best methods for estimating barometric efficiency use many measurements of barometric-pressure change and corresponding water-level change from many time intervals and rely on barometric-pressure-independent water-level change to not be correlated to barometric-pressure change. With many measurements of water-level and barometric-pressure change, the constant relation between ΔW_b and ΔB becomes more apparent while the lack of correlation between ΔW_i and ΔB becomes less apparent.

Systematic Error

Correlation between ΔW_i and ΔB tends to produce a systematic error and, thus, the error ($\Delta W_i/\Delta B$) may be difficult to distinguish from $\Delta W_b/\Delta B$. Such correlation can occur when both the barometric-pressure-independent water-level change and the barometric-pressure change share a common source. Two possible situations that may create correlations between ΔW_i and ΔB are repetitive weather patterns and earth tides.

During repetitive synoptic weather conditions, rain events may occur at similar times with respect to barometric-pressure change. For example, a cold front approaches, barometric pressure decreases, and a rain event causes water levels to rise in the well (ΔW_r); then a high-pressure area moves over the well, and the water level in the well recesses from the rain event. If similar rain events repeatedly occur at about the same time with respect to barometric-pressure fluctuations, the effect of the rain event on ΔW may be difficult to distinguish from the barometric-pressure effect because of the correlation between the rain event and the barometric-pressure change.

Earth tides are nearly semidiurnal (two peaks and two troughs in about 25 hours); atmospheric tides are semidiurnal fluctuations in barometric pressure (two peaks and two troughs in 24 hours). At Air Force Plant 6, diurnal barometric-pressure fluctuations included two daily minima at 3:20 a.m. and 5:20 p.m. and two daily maxima at about 10:30 a.m. and 10:45 p.m. Actual times of the minima and maxima occurred plus/minus an hour. Due to the similar wavelength between atmospheric tides and earth tides, barometric-pressure changes may sometimes correlate to earth-tide fluctuations (ΔW_g) within wells.

Constant Barometric-Pressure-Independent Water-Level Change

A constant barometric-pressure-independent water-level change with time will cause a random error in the estimate of barometric efficiency. For example, long-term water-level trend was a common form of constant barometric-pressure-independent water-level change at Air Force Plant 6. A constant ΔW_i will not correlate to ΔB as long as there is no long-term barometric-pressure trend.

Previous Methods of Estimating the Barometric Efficiency

In this report, four methods of estimating barometric efficiency are compared with the graphical method. This section briefly describes each of these methods, and discusses how they reduce the effect of remaining barometric-pressure-independent water-level change (ΔW_i) during the estimation of barometric efficiency. Discussion emphasizes how the estimation process of each method affects ΔW_i, ΔW_b, and ΔB, and how ΔW_i creates error. A special case of ΔW_i being constant for each time interval (representing long-term trends) also is discussed.

Average-of-Ratios Method

The average of ratios of water-level change to barometric-pressure change ($\Delta W/\Delta B$) for many time intervals can be used as an estimate of barometric efficiency. This method is mathematically simple and also can be used to demonstrate how the effects of barometric-pressure-independent water-level change are reduced during method estimation. Multiplying both sides of equation 7 by $1/\Delta B$ or modifying equation 8 yields:

$$\frac{\Delta W}{\Delta B} = \frac{\Delta W_b}{\Delta B} + \frac{\Delta W_i}{\Delta B} \ . \qquad (10)$$

Expressing equation 10 as the sum of many (n) time intervals yields:

$$\sum_{j=1}^{n} \frac{\Delta W_j}{\Delta B_j} = n\alpha + \sum_{j=1}^{n} \frac{\Delta W_{ij}}{\Delta B_j} \ , \qquad (11)$$

where

$n\alpha$ is $\sum_{j=1}^{n} \Delta W_{bj} / \Delta B_j$, where each $\Delta W_{bj}/\Delta B_j$ is a constant value for every time interval j.

If ΔW_i does not correlate with ΔB, then values of $\Delta W_i/\Delta B$ (error) will be scattered about zero and the sum of many values of $\Delta W_i/\Delta B$ will not be far from zero. Dividing both sides of equation 11 by the number of time intervals (n) yields the "average of ratios" of $\Delta W/\Delta B$:

$$\frac{\sum_{j=1}^{n}\frac{\Delta W_j}{\Delta B_j}}{n} = \alpha + \frac{\sum_{j=1}^{n}\frac{\Delta W_{ij}}{\Delta B_j}}{n}. \quad (12)$$

From equation 12, the average value of $\Delta W/\Delta B$ equals the barometric efficiency plus the average value of $\Delta W_i/\Delta B$. As the number of time intervals increases, the average value of $\Delta W_i/\Delta B$ will approach zero and the average value of $\Delta W/\Delta B$ will be close to the barometric efficiency. This concept is roughly similar to a noise-reduction process that is used in reflection seismics (Yilmaz and Doherty, 1987).

The average of many values of $\Delta W/\Delta B$ will be a reliable estimate of barometric efficiency if there are no large outliers. Outliers of $\Delta W/\Delta B$ will occur within time intervals or increments when (1) ΔB is close to zero or (2) ΔW_i is large. Values of ΔB will be close to zero when a time interval or increment used to determine a value of $\Delta W/\Delta B$ straddles a maximum or minimum of barometric pressure. Values of ΔW_i will be large when a time interval or increment straddles a sudden change in barometric-pressure-independent water level, such as during the beginning of a rain event or aquifer test.

The error in the estimate of barometric efficiency using the average-of-ratios method (ε_{aor}) will be the second term on the right-hand side of equation 12:

$$\varepsilon_{aor} = \frac{\sum_{j=1}^{n}\frac{\Delta W_{ij}}{\Delta B_j}}{n}. \quad (13)$$

From equation 13, it can be seen that one or more time intervals with a ΔB very close to zero will cause a very large error in the estimate of barometric efficiency. Therefore, the average-of-ratios method is vulnerable to any time interval having a small value of ΔB. Confidence intervals of barometric efficiency can be estimated from the spread of values of $\Delta W/\Delta B$ using basic statistical techniques.

In the special case when ΔW_i is constant (*const* W_i) for all time intervals, error in the estimate of barometric efficiency using the average-of-ratios method will be:

$$\varepsilon_{aor} = \frac{\sum_{j=1}^{n}\frac{1}{\Delta B}}{n}\left(const\Delta W_i\right), \quad (14)$$

indicating that if the sum of the reciprocals of values of ΔB for all time intervals is zero, then the average-of-ratios estimate of barometric efficiency will not include error from a constant ΔW_i.

Median-of-Ratios Method

The median-of-ratios method is similar to the average-of-ratios method, except that it uses the median instead of the average as a measure of location. In the case of outliers for $\Delta W/\Delta B$, as previously discussed, a more robust measure of location—such as the median—can provide an estimate that is closer to the barometric efficiency than provided by the average. If ΔW_i does not correlate to ΔB, the probability that $\Delta W_i/\Delta B$ (the error) will be greater than zero will be the same as the probability that the error will be less than zero. As a result, the median for many values of $\Delta W_i/\Delta B$ will be close to zero. Thus, the median value of $\Delta W/\Delta B$ for many time intervals will be close to the value of the barometric efficiency.

Clark Method

The Clark method (Clark, 1967) is presented as a method that can estimate barometric efficiency in the presence of a constant ΔW_i; time intervals are of a constant length. This method has become a standard for comparing other methods or data-processing techniques. Rasmussen and Crawford (1997) compared a version of the Clark method, modified by Davis and Rasmussen (1993), to regression techniques.

The Clark method performs a sign test on ΔW compared to the sign of ΔB for each time interval:

$$\Sigma\Delta W_j = \Sigma\Delta W_{j-1} + \omega_j, \quad (15)$$

where

$\Sigma\Delta W_j$ is the ongoing sum after the j^{th} time interval

and

$\Sigma\Delta W_{j-1}$ is the ongoing sum after the $(j–1)^{th}$ time interval.

The term ω_j is the absolute value of ΔW_j, if the sign of ΔW_j agrees with the sign of ΔB_j (during a specific time interval, water level rises while barometric pressure falls or water level falls while barometric pressure rises); the term ω_j will be the negative of the absolute value of ΔW_j if the sign of ΔW_j disagrees with the sign of ΔB_j (both water level and barometric pressure rise or fall).

If ΔB_j is zero, then ΔW_j is ignored so that changes in water level that occur when there is no change in barometric pressure are eliminated from the estimation of barometric efficiency. With each time interval, the absolute value of ΔB is added to the ongoing sum $\Sigma\Delta B$:

$$\Sigma\Delta B_j = \Sigma\Delta B_{j-1} + \left|\Delta B_j\right|. \quad (16)$$

The estimate of barometric efficiency is the slope of a line that fits $\Sigma\Delta W_j$ plotted on the y-axis and $\Sigma\Delta B$ plotted on the x-axis.

The sign test of ΔW compared to the sign of ΔB from Clark (1967) is a sign test of ΔW_i compared to the sign of ΔB. When the sign of ΔW_i agrees with the sign of ΔB:

$$\omega_j = \left|\Delta W_{bj}\right| + \left|\Delta W_{ij}\right|, \quad (17)$$

when the sign of ΔW_i disagrees with the sign of ΔB:

$$\omega_j = \left|\Delta W_{bj}\right| - \left|\Delta W_{ij}\right|. \quad (18)$$

In the case when the sign of ΔW agrees with the sign of ΔB, (ω is greater than zero) two possible cases exist: (1) the sign of ΔW_i agrees with the sign of ΔB (equation 17) and (2) the sign of ΔW_i disagrees with the sign of ΔB and the absolute value of ΔW_i is less than the absolute value of ΔW_b (equation 18). In the case when the sign of ΔW disagrees with the sign of ΔB and ω is less than zero, the sign of ΔW_i disagrees with the sign of ΔB and the absolute value of ΔW_i is greater than the absolute value ΔW_b (equation 18). It can be seen from equations 15, 17, and 18 that the absolute value of ΔW_b is always added to $\Sigma\Delta W$.

The value of $\Sigma\Delta W/\Sigma\Delta B$ for many (n) time intervals is an estimate of barometric efficiency (also see Davis and Rasmussen, 1993):

$$\hat{\alpha}_n = \frac{\Sigma\Delta W_n}{\Sigma\Delta B_n}. \quad (19)$$

By separating ΔW_i and ΔW_b from ΔW:

$$\frac{\Sigma\Delta W_n}{\Sigma\Delta B_n} = \frac{\Sigma\Delta W_{bn}}{\Sigma\Delta B_n} + \frac{\Sigma\Delta W_{in}}{\Sigma\Delta B_n}, \quad (20)$$

where

$\Sigma\Delta W_{bn}$ is the sum of the absolute values of ΔW_b after n time intervals,

and

$\Sigma\Delta W_{in}$ is the sum of the values of ΔW_i of different signs after n time intervals, with the absolute value of ΔW_i being added when the sign of ΔW_i agrees with the sign ΔB and being subtracted when the sign of ΔW_i disagrees with the sign of ΔB.

If ΔW_i does not correlate to ΔB then about as many time intervals will have the sign of ΔW_i agree with the sign of ΔB (ΔW_i will be added to $\Sigma\Delta W_i$) as will have the sign of ΔW_i disagree with the sign of ΔB (ΔW_i will be subtracted from $\Sigma\Delta W_i$). After many time intervals, $\Sigma\Delta W_i$ will not be far from zero and $\Sigma\Delta W_i/\Sigma\Delta B$ will be insignificant compared to $\Sigma\Delta W_b/\Sigma\Delta B$. The Clark method need not be restricted to time intervals of constant length and need not be performed on a plot of values of $\Sigma\Delta W_j$ on the y-axis and $\Sigma\Delta B_j$ on the x-axis.

The error in the estimate of barometric efficiency using the Clark method will be:

$$\varepsilon_{Clark} = \frac{\Sigma\Delta W_{in}}{\Sigma\Delta B_n}. \quad (21)$$

The estimates of the barometric efficiency converge to a solution when there is little difference in the value of $\Sigma\Delta W/\Sigma\Delta B$ with successive time intervals ($\left(\Sigma\Delta W_j/\Sigma\Delta B_j\right) - \left(\Sigma\Delta W_{j-1}/\Sigma\Delta B_{j-1}\right)$ is close to zero).

In the special case when ΔW_i is constant, error in the estimate of barometric efficiency using the Clark method will be:

$$\varepsilon_{Clark} = \frac{\left(a-d\right) const \Delta W_i}{\Sigma\Delta B_n}, \quad (22)$$

where

a is the number of time intervals when ΔB is greater than zero.

and

d is the number of time intervals when ΔB is less than zero.

The sum of a and d equals n, the total number of time intervals. The estimates of barometric efficiency using the Clark method are resistant to a constant ΔW_i when the number of time intervals with a ΔB of less than zero equals the number of time intervals with a ΔB greater than zero (Davis and Rasmussen, 1993).

Slope Method on Water-Level and Barometric-Pressure Change

Ferris and others (1962) first presented the slope method on ΔW and ΔB from several time intervals. Measures of ΔW are plotted on the y-axis, and those of ΔB are plotted on the x-axis. A line is fitted to the plotted points. The slope of the fitted line is the estimate of barometric efficiency. Using ordinary least squares to obtain an objective best fit of the plotted points, the estimate of barometric efficiency ($\hat{\alpha}$) will be the slope from the ordinary least squares best fit (modified from Ott, 1988):

$$\hat{\alpha} = \frac{S_{\Delta W \Delta B}}{S_{\Delta B \Delta B}}, \quad (23)$$

where

$$S_{\Delta W \Delta B} = \sum_{j=1}^{n}\left(\Delta W_j - \overline{\Delta W}\right)\left(\Delta B_j - \overline{\Delta B}\right) \quad (24)$$

and

$$S_{\Delta B \Delta B} = \sum_{j=1}^{n}\left(\Delta B_j - \overline{\Delta B}\right)^2, \quad (25)$$

where

j designates the j^{th} time interval;

$\overline{\Delta W}$ is the average water-level change for all time intervals;

and

$\overline{\Delta B}$ is the average barometric-pressure change for all time intervals.

The r-squared value will provide information about the scatter of the plotted points and the reliability of the estimate of barometric efficiency.

As with other methods, replacing ΔW with ΔW_i will yield the error in the estimate of barometric efficiency:

$$\varepsilon_{slope} = \frac{S_{\Delta W_i \Delta B}}{S_{\Delta B \Delta B}} , \qquad (26)$$

where

$$S_{\Delta W_i \Delta B} = \sum_{j=1}^{n} \left(\Delta W_{ij} - \overline{\Delta W_i} \right) \left(\Delta B_j - \overline{\Delta B} \right) . \qquad (27)$$

The error in the estimate of barometric efficiency is then the slope of ΔW_i as a function of ΔB. The larger the sample size, the lower the probability that ΔW_i (not correlated to ΔB) will plot against ΔB as a slope that is significantly different from zero.

In the special case that ΔW_i is constant, the slope of ΔW_i as a function of ΔB will be zero. Therefore, a constant ΔW_i will not cause error in the estimate of barometric efficiency using the slope method. The constant ΔW_i will be expressed as the y-intercept of the ordinary least squares calculation.

Some estimates of barometric efficiency use the slope method with water level (*W*) on the y-axis and barometric pressure (*B*) on the x-axis (Hare and Morse, 1999). The negative of the slope of the best-fit line through points of water level (*W*) plotted against barometric pressure (*B*) is the estimate of barometric efficiency. It is advisable to use ΔW and ΔB in the slope method rather than *W* and *B* because ΔW and ΔB are more mathematically accurate (barometric efficiency is defined as the ratio of water-level change to barometric-pressure change, not water level to barometric pressure). Plots of ΔW and ΔB, also, show less scatter, compared to plots of *W* and *B* (see fig. 2 for an example).

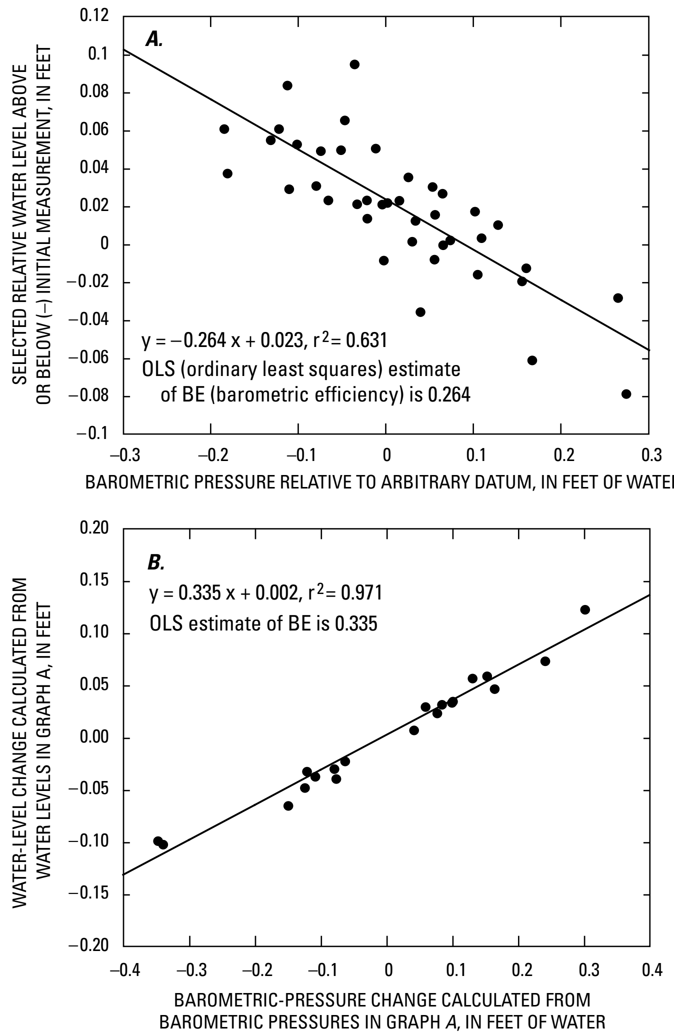

Figure 2. *(A)* Selected water-level values as a function of barometric pressure and *(B)* water-level change as a function of barometric-pressure change in well mwg05, Air Force Plant 6, Marietta, Georgia, 2003. See figure 1 for well location.

Using Continuous Data to Estimate Barometric Efficiency

With advances in data-collection equipment, continuous data are more readily available. A graphical method was developed that uses continuous water-level and barometric-pressure data to estimate barometric efficiency. Continuous data provide more information than discrete data to estimate the barometric efficiency. Continuous data in this report are actually "nearly continuous" data where the parameter resolution and sample frequency are great enough to define the shape of barometric-pressure and water-level fluctuations through time. This section of the report (1) describes simple techniques for removing some of the barometric-pressure-independent water-level change from the water-level data prior to using a method to estimate the barometric efficiency, and (2) discusses the optimal selection of time intervals from time-series data.

Filtering Water-Level Change that Causes Error in the Estimation of Barometric Efficiency

Simple techniques exist for removing barometric-pressure-independent water-level change related to time—long-term water-level change and daily fluctuations. While discussion in this report is limited to these two forms of barometric-pressure-independent water-level change, other forms that can be quantified should be removed.

Decreasing the variance of water-level data by correcting the data with an independent variable that is not correlated to barometric pressure will decrease the amount of barometric-pressure-independent water-level change in the water-level data. The reduction in barometric-pressure-independent water-level change from the water-level data can be monitored by comparing the variance in corrected water-level data to the variance in uncorrected water-level data.

Long-Term Barometric-Pressure-Independent Water-Level Change

Long-term barometric-pressure-independent water-level change (ΔW_i) can be identified from a water-level hydrograph if the following criteria are met: (1) the time length of the trend is much longer than the time length of barometric-pressure fluctuations, (2) barometric pressure lacks a long-term trend, and (3) the water-level trend is easily identifiable and can be represented by a simple mathematical expression. Barometric-pressure fluctuations during the aquifer-test period at Air Force Plant 6 ranged from 1 to 7 days. Long-term water-level trends extended for the length of the study period, which was at least 60 days. At Air Force Plant 6, barometric pressure fluctuated about an average value, exhibiting no long-term trend.

Examples of correcting for a linear change (constant rate of change), and a second-order, parabolic trend (increase to a maximum water level followed by a decrease) are described below. Data corrections decrease some barometric-pressure-independent water-level change using time as the independent variable. Conceptually, a simple shape (line or parabola) that represents the long-term trend is fitted and subtracted from the water-level data. The resulting residual of the trend is corrected data with a variance in water level that is smaller than the variance in water level from the uncorrected data. Optimal correction factors provide the minimum variance in corrected water level. The smaller the variance of water level, the more horizontal the curve of water level as a function of time.

In the linear trend, water-level change is constant with time. The correction formula is:

$$W_{(t)corr} = W_{(t)uncorr} - \tau\left(t - t_0\right) , \qquad (28)$$

where

$W_{(t)corr}$ is the water level at time t corrected for a long-term linear trend;

$W_{(t)uncorr}$ is the uncorrected water level at time t;

and

τ is the rate of water-level change per unit of time determined by ordinary least squares.

Figure 3 shows an example of correcting a well hydrograph for a linear, long-term trend (well b4mwi). Table 1 lists variances of the 6,411 uncorrected and corrected water-level values. Correcting the water-level data with a value for τ of –0.0153, the water-level variance is decreased from 0.08954 to 0.00290, reducing more than 95 percent of the variance. The resulting hydrograph of corrected water level shows little to no long-term trend (is horizontal) yet retains other water-level features within the graph (fig. 3).

In the second-order, parabolic trend, the correction formula is:

$$W_{(t)corr} = W_{(t)uncorr} + \frac{\left(t - t_v\right)^2}{4p} , \qquad (29)$$

where

t_v is the time when the long-term water level reaches a maximum or minimum value (the maximum value in the example in this report)

and

p is a parameter that is adjusted to remove the trend.

Figure 4 shows an example of correcting a well hydrograph for a second-order, long-term trend (well pmw7d). Table 1 lists variances of the 6,412 15-minute uncorrected and corrected water-level values. Correcting the water-level data with a value for p of 1,950, the water-level variance is decreased from 0.00425 to 0.00138, reducing more than 65 percent of the variance. The resulting hydrograph of corrected water level shows no long-term trend (is horizontal) yet retains other water-level features within the graph (fig. 4).

Daily Fluctuations

Some short-term fluctuations can be removed using a frequency filter or by using a centered daily-moving arithmetic mean (hereinafter, the arithmetic mean is referred to as the average). Geldon and others (1997) used a low-pass Butterworth filter to remove water-level fluctuations with frequencies of greater than 0.8 cycles per day. Centered daily-moving averages of both the barometric pressure and water level also can remove daily fluctuations that interfere with estimations of barometric efficiency. Centered daily-moving average at each time increment (for example, 15 minutes) is the average water level or barometric pressure for all time increments during a 24-hour

Table 1. Variance of corrected water-level data using selected values of correction factors for two wells, b4mwi and pmw7d, Air Force Plant 6, Marietta, Georgia, 2003.

[n, sample size or number of 15-minute measurements of water level, amounting to a study period of about 67 days; τ, correction factor used in correcting for a linear, long-term trend; –, negative; NA, not applicable; p, correction factor used in correcting for a second-order, parabolic, long-term trend]

Variable name or description	Well name	
	b4mwi	**pmw7d**
Sample size (n)	6,411	6,412
Variance of uncorrected water levels	0.08954	0.00425
Trend	Linear	Second-order parabolic
Selected value of τ	–0.0153	NA
Selected value of p	NA	1,950
Variance of corrected water levels	0.00290	0.00138

period with the time increment in the center of the period. As an example, if continuous recorders are measuring barometric pressure and water level every 15 minutes, the daily-moving-average value for the time March 5 at 10:15 a.m. will be the average barometric pressure and the average water level for all 97 15-minute intervals starting March 4 at 10:15 p.m. through March 5 at 10:15 p.m. The daily-moving-average values for the time March 5 at 10:30 a.m. will be the average barometric pressure and the average water level for all 97 15-minute intervals starting March 4 at 10:30 p.m. through March 5 at 10:30 p.m. Daily-moving averages are very easy to apply to time-series data and are effective in removing daily water-level fluctuations. As long as daily-moving averages are applied to both the barometric-pressure and water-level values, there appears to be no adverse effect on the estimation of barometric efficiency for long-term barometric-pressure fluctuations on the scale of days. Because earth-tide fluctuations (ΔW_g) cycle slightly longer than 24 hours, it may be advisable to extend the time used for daily-moving averages to slightly longer than 24 hours.

It should be confirmed that no time lag in barometric effects are present, prior to using filters or daily-moving averages to reduce short-term fluctuations in barometric pressure or water level. If a time lag is present, depending on the scope of the study, barometric efficiency may need to be estimated at more than one time scale (Toll and Rasmussen, 2007). While the centered daily-moving average water level is used to estimate barometric efficiency, it is not used to calculate drawdown in a well for an aquifer test.

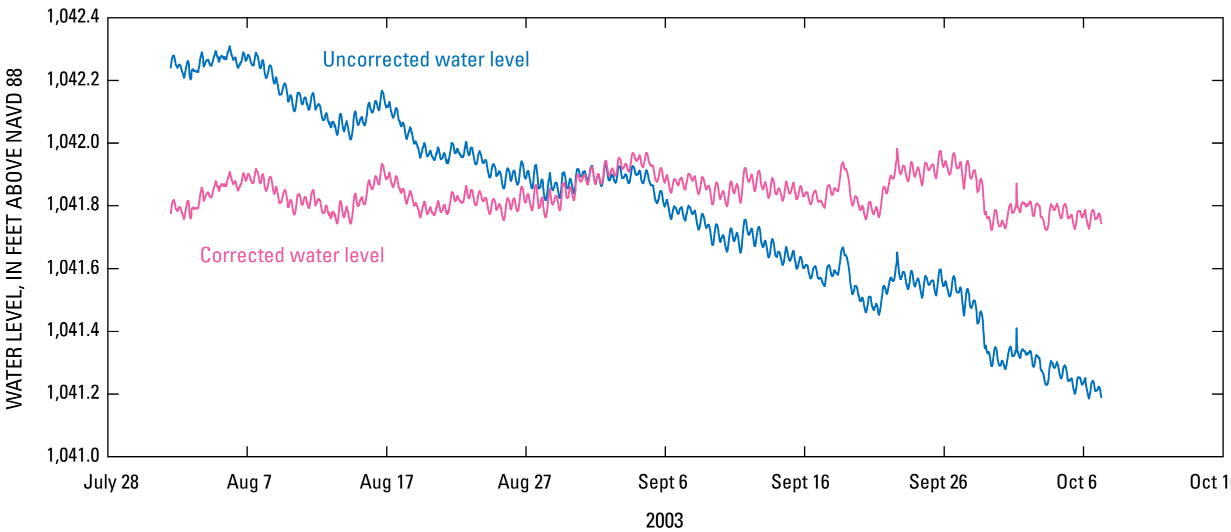

Figure 3. Example of removing barometric-pressure-independent water-level change in the form of long-term linear trend, well b4mwi, Air Force Plant 6, Marietta, Georgia, 2003.

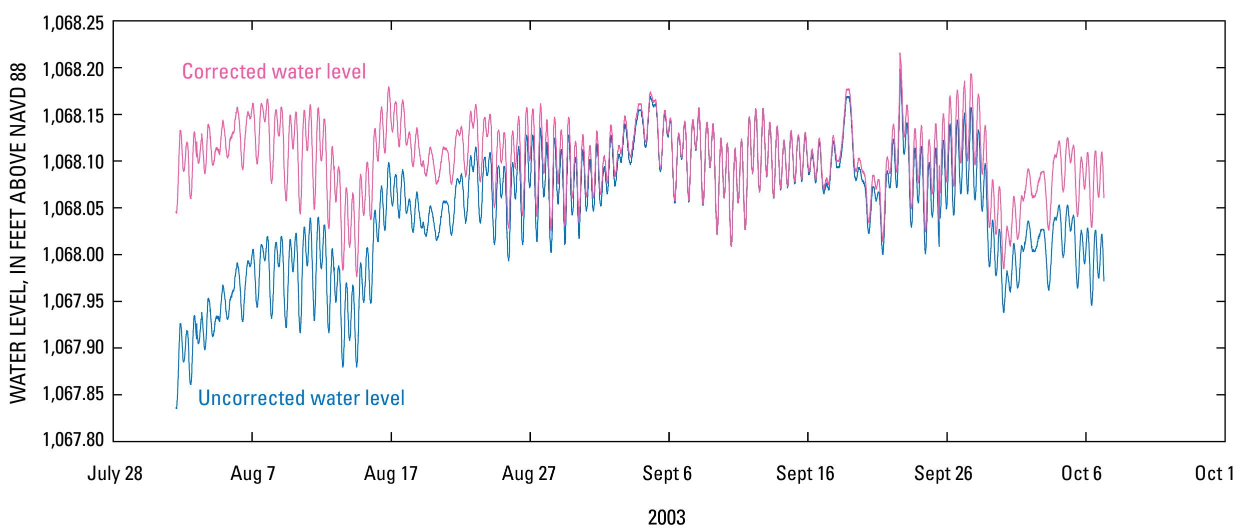

Figure 4. Example of removing barometric-pressure-independent water-level change in the form of long-term 2nd-order, parabolic trend, well pmw7d, Air Force Plant 6, Marietta, Georgia, 2003.

Other Barometric-Pressure-Independent Water-Level Changes

As long as an identified trend does not correlate to barometric pressure, and it can be feasibly quantified, it should be removed prior to barometric-efficiency estimation. Recession curves after rain events (ΔW_r), earth tides (ΔW_g), and ocean tides (ΔW_m) are examples of other barometric-pressure-independent water-level change that might be removable from data prior to estimating barometric efficiency. Methods discussed in this report can be applied to earth-tide fluctuations to determine tidal efficiency by using one of the directional components of microgravity as the independent variable. Tidal efficiency then can be used to correct water-level data for earth tides prior to determining barometric efficiency.

Time-Interval Selection

Methods described in the previous section require that ΔW and ΔB be measured for multiple time intervals. Time intervals should be selected such that the value of ΔW_i is as small as possible compared to the value of ΔB, as is reflected in equation 9.

One way to optimize the quality of data in the time intervals is to focus on the inflection points of barometric-pressure fluctuations (fig. 5). Such inflection points are those times when the barometric pressure is changing most rapidly. If ΔW_i does not correlate to ΔB, then the rate of change of W_i ($\Delta W_i / \Delta T$) will not correlate to the rate of change of B ($\Delta B/\Delta T$). As a result, focusing time-interval selection about these inflection points will maximize the value of ΔB while not maximizing the value of ΔW_i. The result will be that time intervals will have minimum values of $\Delta W_i / \Delta B$ (error) associated with them.

Time-interval boundaries are selected so that they are close enough to the inflection point to obtain the benefit of rapidly-changing barometric pressure but far enough apart to ensure that the barometric-pressure change associated with the time interval is significantly greater than measurement error. Time-interval-boundary selection becomes important when the shapes of barometric-pressure fluctuations, in time series, are not simple. Features to avoid include times when barometric pressure is slowly changing during a relatively long period of time. The boundaries for optimally selected time intervals will be situated between the inflection points and the extremes of the barometric-pressure fluctuation (for example, one boundary is between the minimum and an inflection point and the other boundary is between the inflection point and the maximum).

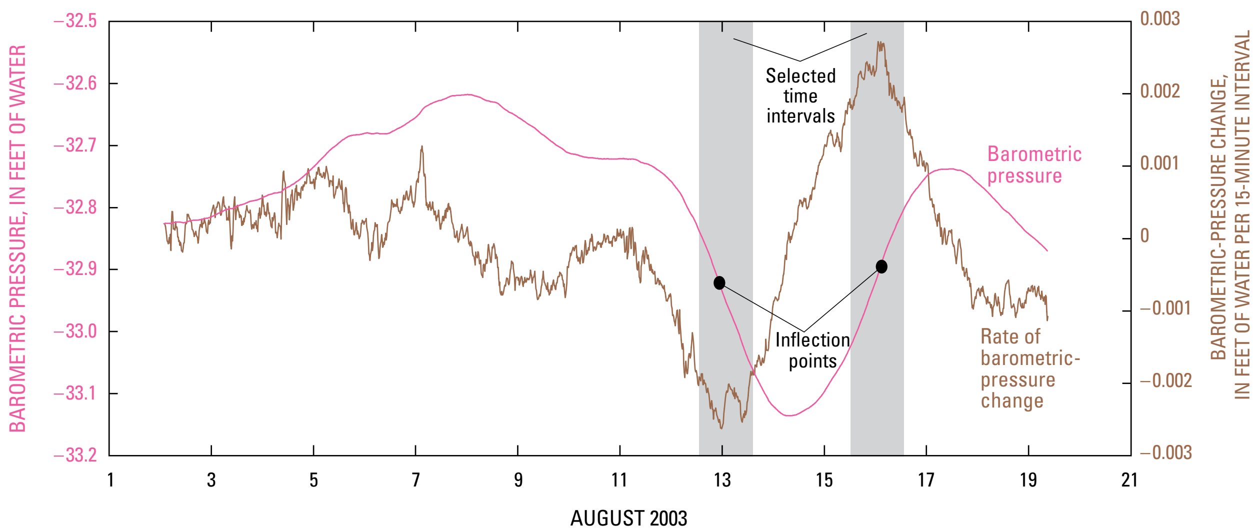

Figure 5. Example of time-interval selection about two inflection points during maximum rates of barometric-pressure change, well b4mwi, Air Force Plant 6, Marietta, Georgia, August, 2003. Barometric pressure is in the form of daily-moving averages.

A Graphical Method for Estimating Barometric Efficiency from Continuous Water-Level Data

This section describes a graphical method that uses continuous data to quickly determine if water levels are affected by barometric-pressure change and to estimate barometric efficiency in a manner that is resistant to large barometric-pressure-independent water-level change. This section (1) discusses the theory behind the graphical method, (2) presents examples from actual continuous data of graphical features used to estimate the barometric efficiency, (3) describes two techniques for determining barometric efficiency from continuous data using the graphical method, and (4) provides an example application in the Piedmont at Air Force Plant 6, Marietta, Georgia.

Theory Behind the Graphical Method

A plot of nearly continuous water level (on the y-axis) as a function of nearly continuous barometric pressure (on the x-axis) will plot as a line curved into a series of connected elliptical loops (figs. 6–10). A complete fluctuation in barometric pressure, in time series (from minimum to maximum back to minimum, or from maximum to minimum back to maximum, fig. 6*A*), plots as a single loop (parabolic if open or elliptical if closed) on a graph of water level as a function of barometric pressure (closed loop in fig. 6*B*; open and closed loops in fig. 7*B*). Hereinafter loop shapes will be called elliptical.

The length of an elliptical loop seen on the graph, along the horizontal x-axis, can be mathematically represented as a compilation of two barometric-pressure changes ($\overline{\overline{\Delta B}}$). The double-bar over ΔB is used here to indicate that each value of change comes from four barometric-pressure values as shown in equation 30:

$$\overline{\overline{\Delta B_j}} = \frac{1}{2}\left[\left(B_{j1} + B_{j4}\right) - \left(B_{j2} + B_{j3}\right)\right], \qquad (30)$$

where

j is for the j^{th} barometric-pressure fluctuation or loop

and

B_{j1}, B_{j2}, B_{j3}, and B_{j4} are values of barometric pressure at times t_1, t_2, t_3, and t_4, respectively.

Parts of a loop that are most apparent on a graph originate from barometric-pressure data that best estimates barometric efficiency. The four times in equation 30 (t_1, t_2, t_3, and t_4) are times that best define the slope of the loop as it appears on a graph. These four times happen to occur at the boundaries of times during which the barometric-pressure change is most rapid. As discussed in a previous section, time t_1 occurs between the first maximum or minimum and the first inflection point, time t_2 occurs between the first inflection point and the intermediate minimum or maximum, time t_3 occurs between the intermediate minimum or maximum and the second inflection point, and time t_4 occurs between the second inflection point and the second maximum or minimum (fig. 6).

The length of an elliptical loop seen on the graph, along the vertical y-axis, can be mathematically represented as a compilation of two water-level changes ($\overline{\overline{\Delta W}}$) and can be calculated as follows:

$$\overline{\overline{\Delta W_j}} = \frac{1}{2}\left[\left(W_{j2} + W_{j3}\right) - \left(W_{j1} + W_{j4}\right)\right], \qquad (31)$$

where

W_1, W_2, W_3, and W_4 are water levels during the same times as B_1, B_2, B_3, and B_4, respectively.

The order of times t_1 and t_4, and t_2 and t_3 in equation 30 is inverted with respect to equation 31 in order to follow the convention that an increase in barometric pressure is a negative change during a time interval.

The plots of continuous data are for water level as a function of barometric pressure. As a result, the negative of the slopes of the elliptical loops on the graph will be the water-level change divided by the barometric-pressure change ($\overline{\overline{\Delta W}}/\overline{\overline{\Delta B}}$) that is associated with barometric-pressure fluctuations.

Using figure 6 as an example, a barometric-pressure fluctuation occurs such that there is a first barometric-pressure minimum, time t_1, an inflection point, time t_2, an intermediate barometric-pressure maximum, time t_3, another inflection point, time t_4, and a second barometric-pressure minimum. The negative of the slope of the long axis of an elliptical loop will be $\overline{\overline{\Delta W}}/\overline{\overline{\Delta B}}$ or from equation 10 will be the sum of two ratios: $\overline{\overline{\Delta W_b}}/\overline{\overline{\Delta B}}$ (the barometric efficiency) and $\overline{\overline{\Delta W_i}}/\overline{\overline{\Delta B}}$ (the error). Values of $\overline{\overline{\Delta W}}/\overline{\overline{\Delta B}}$ usually vary for each loop (barometric-pressure fluctuation).

The negative of the slope of the preferred orientation of many elliptical loops, as viewed by an observer, is an estimate of barometric efficiency. The slope of the preferred orientation of many elliptical loops is approximately the median of the slopes of the major axes of the elliptical loops. The graphical method uses the same principle used in the median-of-ratios method; however, instead of using direct ratios from time intervals in the median-of-ratios method, negative*s* of the slopes of loops are used in the graphical method. The error in the estimate of barometric efficiency using the graphical method (ε_{gm}) will be:

$$\varepsilon_{gm} = median\left(\overline{\overline{\Delta W_{ij}}}/\overline{\overline{\Delta B_j}}\right), \qquad (32)$$

plus observational error.

Observational error is defined as the difference between the preferred orientation of the slopes of the loops as determined by the observer, and the actual median of the slopes of the loops. Because there is observational error, it is advisable that more than one person select the slope or that the same person selects the slope for the same data several times in order to minimize the effect of subjectivity. Also a long study period should be used (at least 60 days) to ensure that the loops that are affected by large amounts of ΔW_i do not significantly contribute error to the barometric-efficiency estimate.

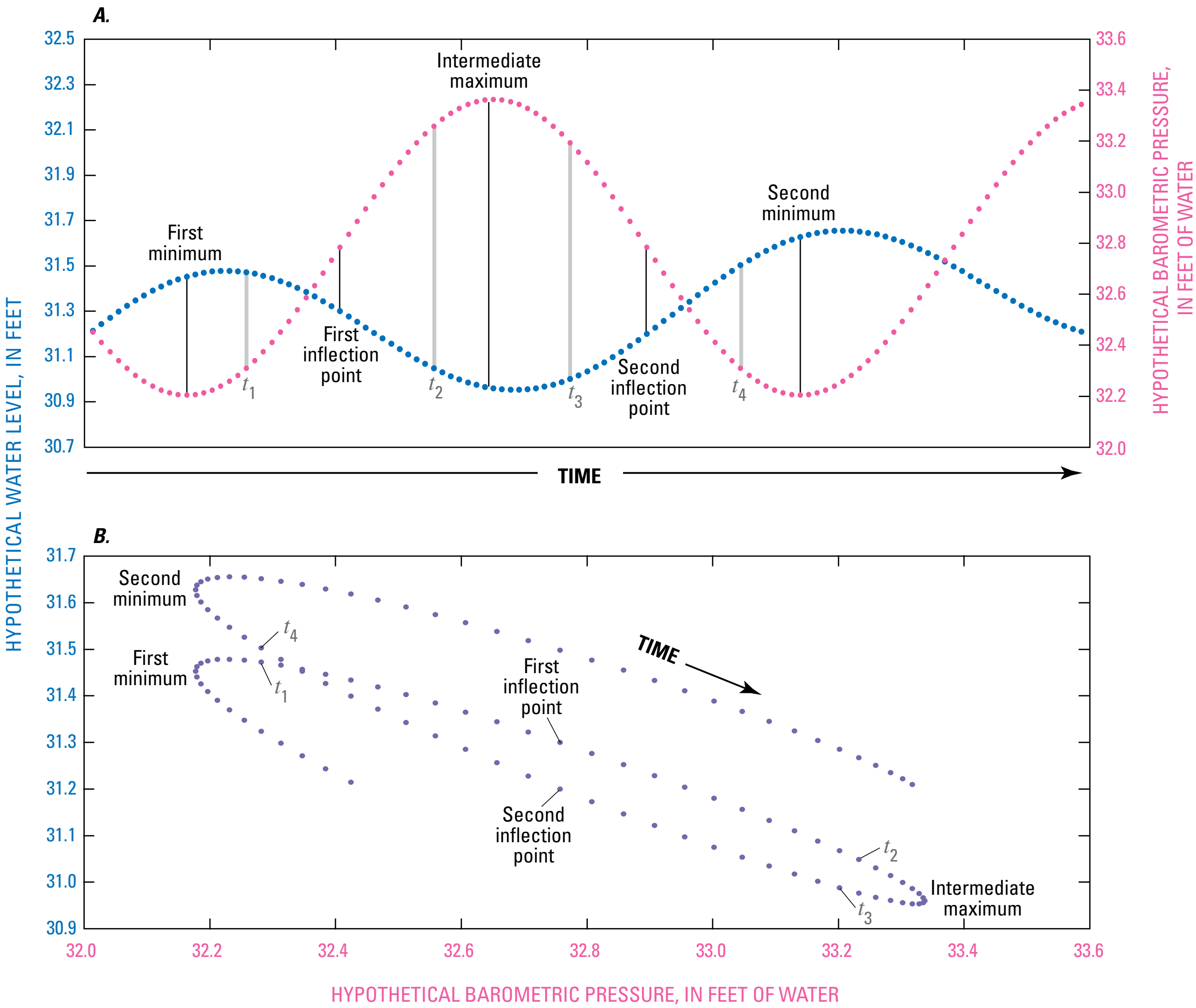

Figure 6. Example of *(A)* time series of hypothetical water level and barometric pressure, and *(B)* hypothetical water level as a function of barometric pressure. Barometric efficiency equals 0.50.

If there is a constant barometric-pressure-independent water-level change with time at a rate of τ, $\overline{\overline{\Delta W_i}}$ will originate from an asymmetry in the barometric-pressure fluctuation with respect to time. Replacing $\overline{\overline{\Delta W}}$ with $\overline{\overline{\Delta W_i}}$ in equation 31:

$$\overline{\overline{\Delta W_{ij}}} = \frac{1}{2}\left[\left(W_{ij2} + W_{ij3}\right) - \left(W_{ij1} + W_{ij4}\right)\right], \qquad (33)$$

where

W_{i1}, W_{i2}, W_{i3}, and W_{i4} are water levels that are not caused by barometric-pressure change during the same times as B_1, B_2, B_3, and B_4, respectively.

If $(t_2 - t_1)$ and $(t_4 - t_3)$ are the same for a specified barometric-pressure fluctuation, that is, the time intervals about the inflection points or "limbs" of the loop are the same with respect to time, and the rate of barometric-pressure-independent water-level change is constant, $\overline{\overline{\Delta W_i}}$ will be zero. If the limbs of the loop are not equal and the rate of barometric-pressure-independent water-level change is constant, the value of $\overline{\overline{\Delta W_i}}$ will be half of the difference in the time between the two limbs multiplied by the rate of barometric-pressure-independent water-level change with time (τ). Therefore, in the special case of a constant barometric-pressure-independent water-level change (*const*-ΔW_i in other methods), the error in the estimate of barometric efficiency using the graphical method will be:

$$\varepsilon_{gm} = median\left(\frac{\frac{\tau}{2}\left[\left(t_{j2} + t_{j3}\right) - \left(t_{j1} + t_{j4}\right)\right]}{\overline{\overline{\Delta B_j}}}\right), \qquad (34)$$

plus observational error. The term

j is for the j^{th} barometric-pressure fluctuation;

t_1, t_2, t_3, and t_4 are times as used in equations 30, 31, and 33;

τ is the rate of barometric-pressure-independent water-level change with time;

and

$\overline{\overline{\Delta B_j}}$ is the barometric-pressure change as defined in equation 30.

Examples of Elliptical Loops in Graphs

Determining the slope of the preferred orientation of loops requires data frequency to be high enough that shapes of the water-level and barometric-pressure fluctuations are defined by the data. Figures 7*A*–10*A* are time-series plots of water level and barometric pressure for select wells at Air Force Plant 6. Figures 7*B*–10*B* are plots of nearly continuous water level as a function of nearly continuous barometric pressure. Long-term trends have been removed. Data presented in this report are in the form of centered daily-moving averages.

Figure 7 shows fluctuations of barometric pressure and water level of a well (ob202b) with a barometric efficiency as estimated from the graphical-loop method of 0.703. In the time-series graph (fig. 7*A*), there is a correlation between barometric-pressure changes and water-level changes. Peaks and troughs of water level tend to coincide with troughs and peaks of barometric pressure, respectively. A plot of nearly continuous water level as a function of barometric pressure (fig. 7B) shows several loops, each representing a barometric-pressure fluctuation. The slopes of the loops vary slightly, with a slope of the preferred orientation of −0.703.

Figure 8 shows the fluctuations of barometric pressure and water level of a well (mwg05) with a barometric efficiency as estimated by the graphical-loop method of 0.379. Although the barometric efficiency is lower than that of well ob202b, the time-series graph (fig. 8*A*) still shows a correlation between barometric pressure and water level. Peaks and troughs of water levels from well mwg05 are smaller than those of well ob202b; however, they still tend to coincide with barometric-

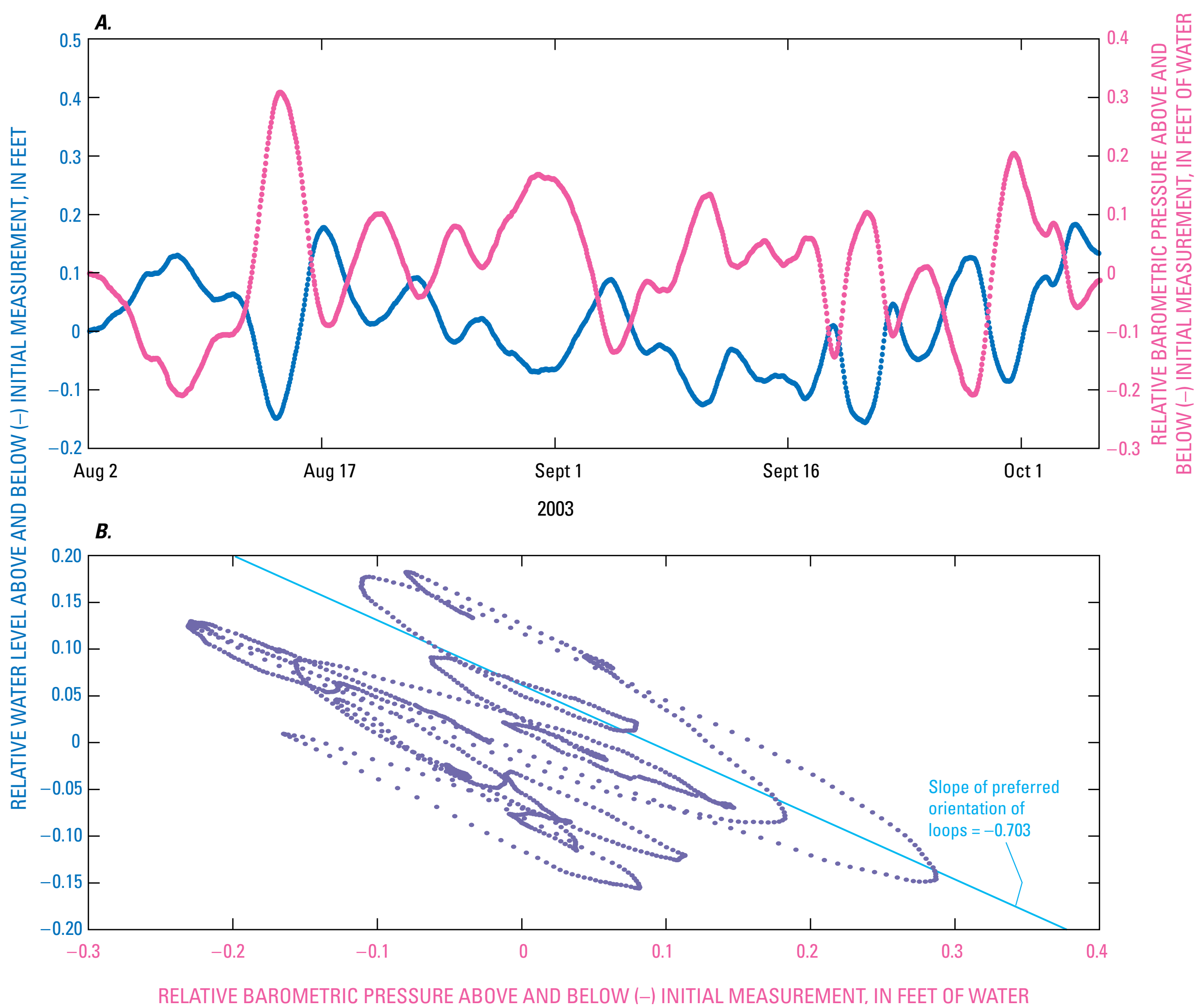

Figure 7. *(A)* Time series of water level and barometric pressure, and *(B)* water level as a function of barometric pressure for well ob202b, August 2–October 6, 2003. Barometric-efficiency estimate from the graphical method is 0.703; initial water-level and barometric-pressure measurements are normalized to zero. Data are in the form of daily-moving averages. See figure 1 for well location.

pressure troughs and peaks, respectively. The plot of nearly continuous water level as a function of barometric pressure (fig. 8*B*) shows most of the loops nested within one large loop. Most of the loops have a slope close to the slope of the preferred orientation of –0.379.

Figure 9 shows fluctuations of barometric pressure and water level of a well (ob208c) with a barometric efficiency as estimated by both the Clark (1967) method and the graphical-loop method near 0.16. In the time-series graph (fig. 9*A*), the correlation between water level and barometric pressure is not apparent. The plot of nearly continuous water level as a function of barometric pressure (fig. 9*B*) shows a number of loops with a slope of preferred orientation of –0.162. A rain event near September 22, 2003, is apparent in figure 9A as a spike, and in figure 9*B* as a loop with a different slope than those of other loops. Thus, the slope of the loop from the rain event is ignored in the analysis.

Figure 10 shows fluctuations of barometric pressure and water level of a well (mwg11) under strong surface influence and with a barometric efficiency of near zero. The barometric efficiency estimated by the graphical method was 0.027. In the time-series graph (fig. 10*A*), well mwg11 responds to rain events. No correlation is apparent between the water level and barometric pressure. In the plot of nearly continuous water level as a function of barometric pressure (fig. 10*B*), most of the loops have a preferred orientation that is nearly horizontal. The slope of the preferred orientation of the loops was measured as –0.027. Several loops have a positive slope ($\overline{\overline{\Delta W}}/\overline{\overline{\Delta B}}$ less than zero). The positive sloping loops are the result of rainfall events (spike in water level followed by a lengthy recession curve) coinciding with some barometric-pressure changes (fig. 10*A*).

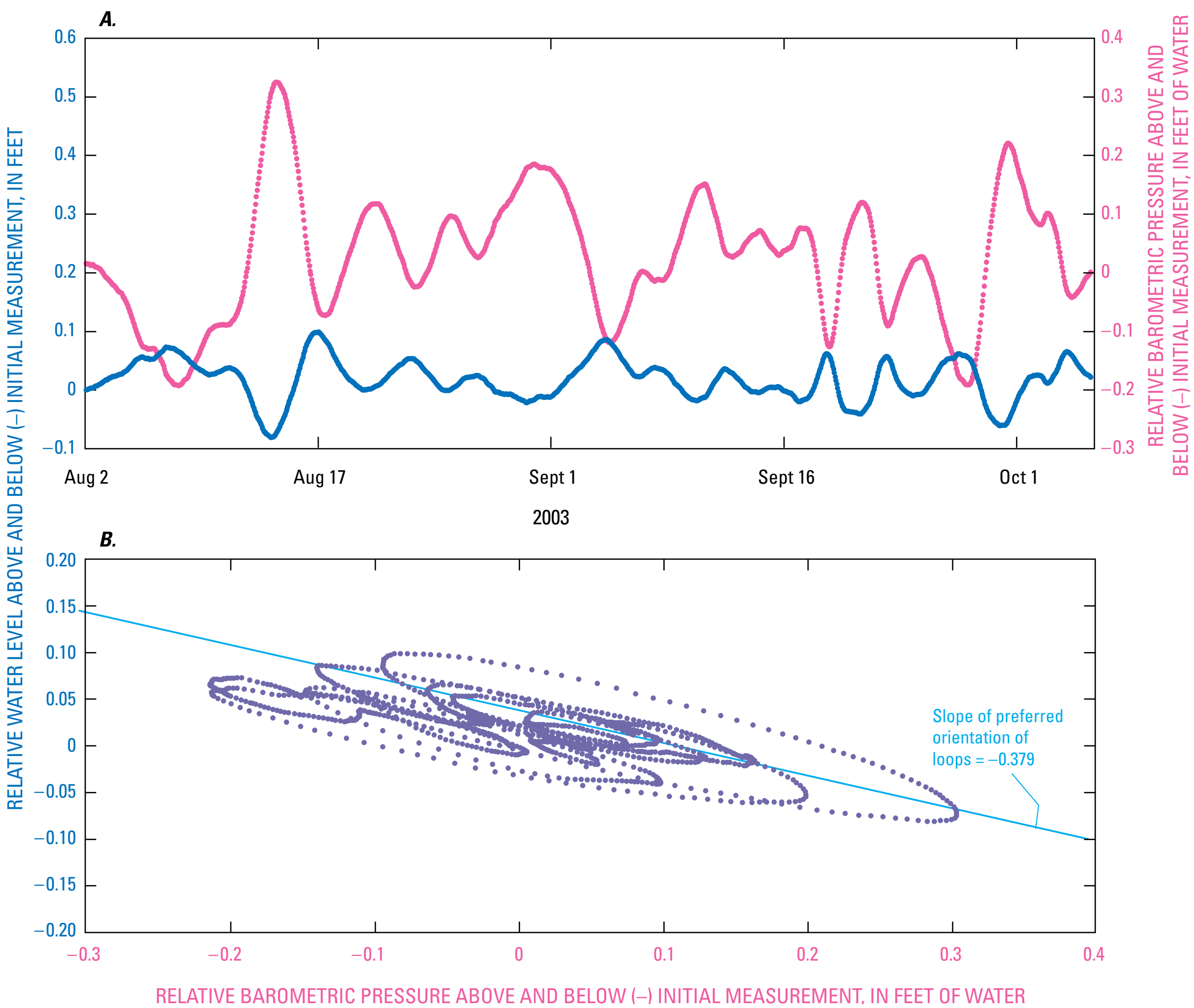

Figure 8. *(A)* Time series of water level and barometric pressure, and *(B)* water level as a function of barometric pressure for well mwg05, August 2–October 6, 2003. Barometric-efficiency estimate from the graphical method is 0.379; initial water-level and barometric-pressure measurements are normalized to zero. Data are in the form of daily-moving averages. See figure 1 for well location.

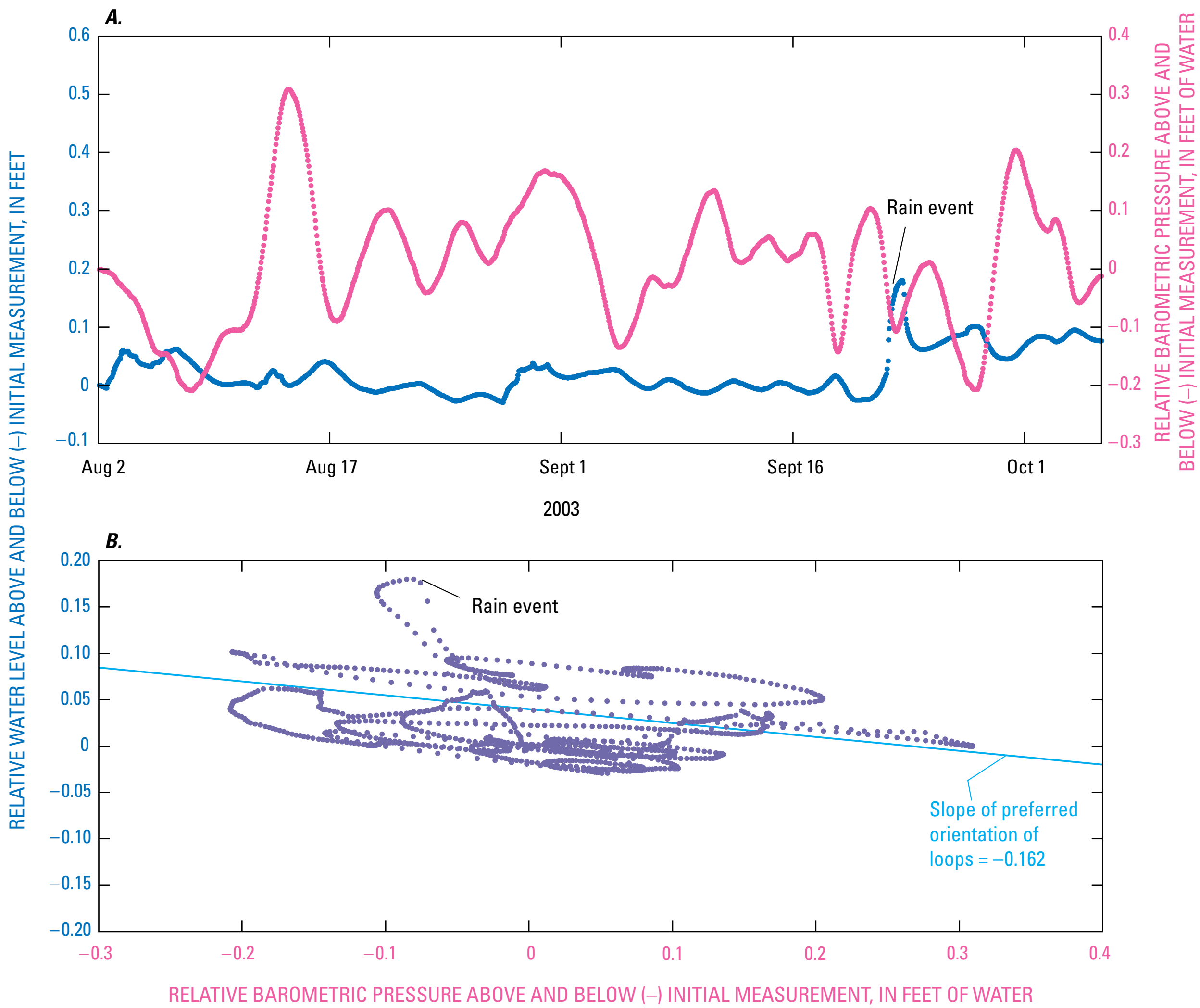

Figure 9. *(A)* Time series of water level and barometric pressure, and *(B)* water level as a function of barometric pressure for well ob208c, August 2–October 6, 2003. Barometric-efficiency estimate from the graphical method is 0.162; initial water-level and barometric-pressure measurements are normalized to zero. Data are in the form of daily-moving averages. See figure 1 for well location.

Determining the Slope of the Preferred Orientation of Loops

Two techniques to determine the slope of the preferred orientation of all loops within a given graph are presented herein. The first technique is to orient a straight line parallel to the preferred orientation of the loops (straight lines in figs. 7*B*, 8*B*, 9*B*, and 10*B*). The negative of the slope of the straight line is the estimate of barometric efficiency. The second technique is to adjust a correction factor to modify the slope of the preferred orientation of the loops of corrected water level as a function of barometric pressure. The correction factor that modifies the slope to zero is the estimate of barometric efficiency. The second technique is discussed in detail below.

The second technique uses a spreadsheet and an accompanying graph. Figure 11*A* shows the spreadsheet including a graph, on the right side of the spreadsheet, which is a plot of nearly continuous, centered daily-moving-average water level as a function of nearly continuous, centered daily-moving-average barometric pressure. Loops with a preferred orientation are apparent on the graph. The slope of the preferred orientation of the loops is less than zero, indicating that the well is noticeably affected by barometric-pressure change.

The columns within the spreadsheet (fig. 11*A*) are date and time (columns A and B, respectively); barometric pressure, in feet of water, and centered daily-moving average of barometric pressure (columns D and E, respectively); water level in well ob202b (column G); water level after being

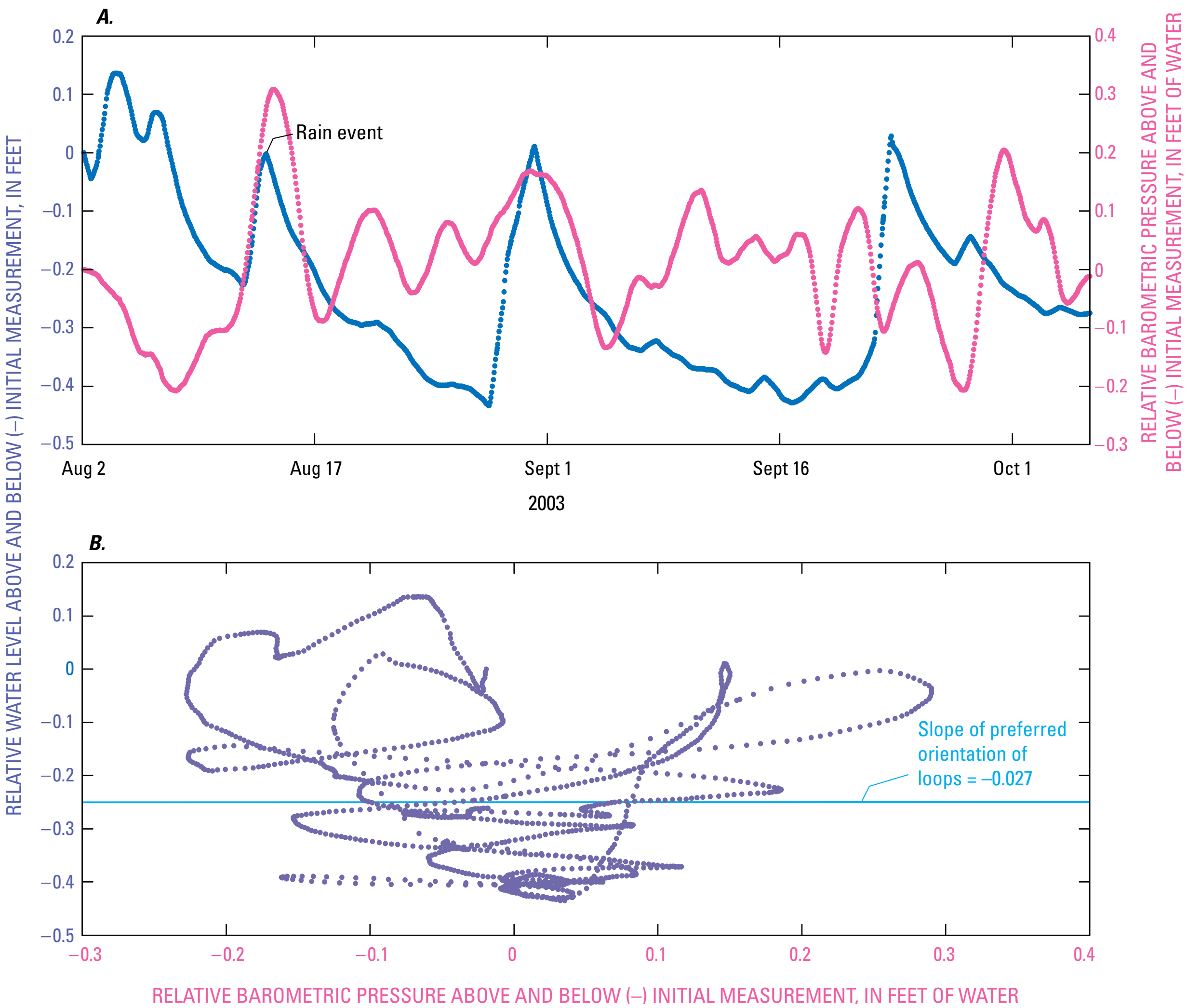

Figure 10. *(A)* Time series of water level and barometric pressure, and *(B)* water level as a function of barometric pressure for well mwg11, August 2–October 6, 2003. Barometric-efficiency estimate from the graphical method is 0.027; initial water-level and barometric-pressure measurements are normalized to zero. Data are in the form of daily-moving averages. See figure 1 for well location.

corrected for a long-term trend (column I); water level from column I that is "corrected" for barometric-pressure change using a proposed value of barometric efficiency (column J); and, finally, centered daily-moving average of water level from column J (column K). Columns C, F, and H are blank. Data from columns E and K are not visible on fig. 11*A*.

Each cell in column J has the following formula derived from equation 3:

$$W_{(j)} = W_{(j)uncorr} - m\left(B_0 - B_{(j)}\right), \qquad (35)$$

where

j is for the j^{th} row (related to a 15-minute interval);

$W_{(j)}$ is the water level, in column J;

$W_{(j)uncorr}$ is the water level that has been corrected for a long-term trend but has not been corrected for barometric pressure, in column I;

m is the proposed barometric efficiency, input into cell J2;

$B_{(j)}$ is the barometric pressure, in column D;

and

B_0 is the reference barometric pressure (32.836 feet of water).

With the correction factor m (cell J2) set to zero, the graph is inspected and is determined to have a preferred orientation of loops with a negative slope.

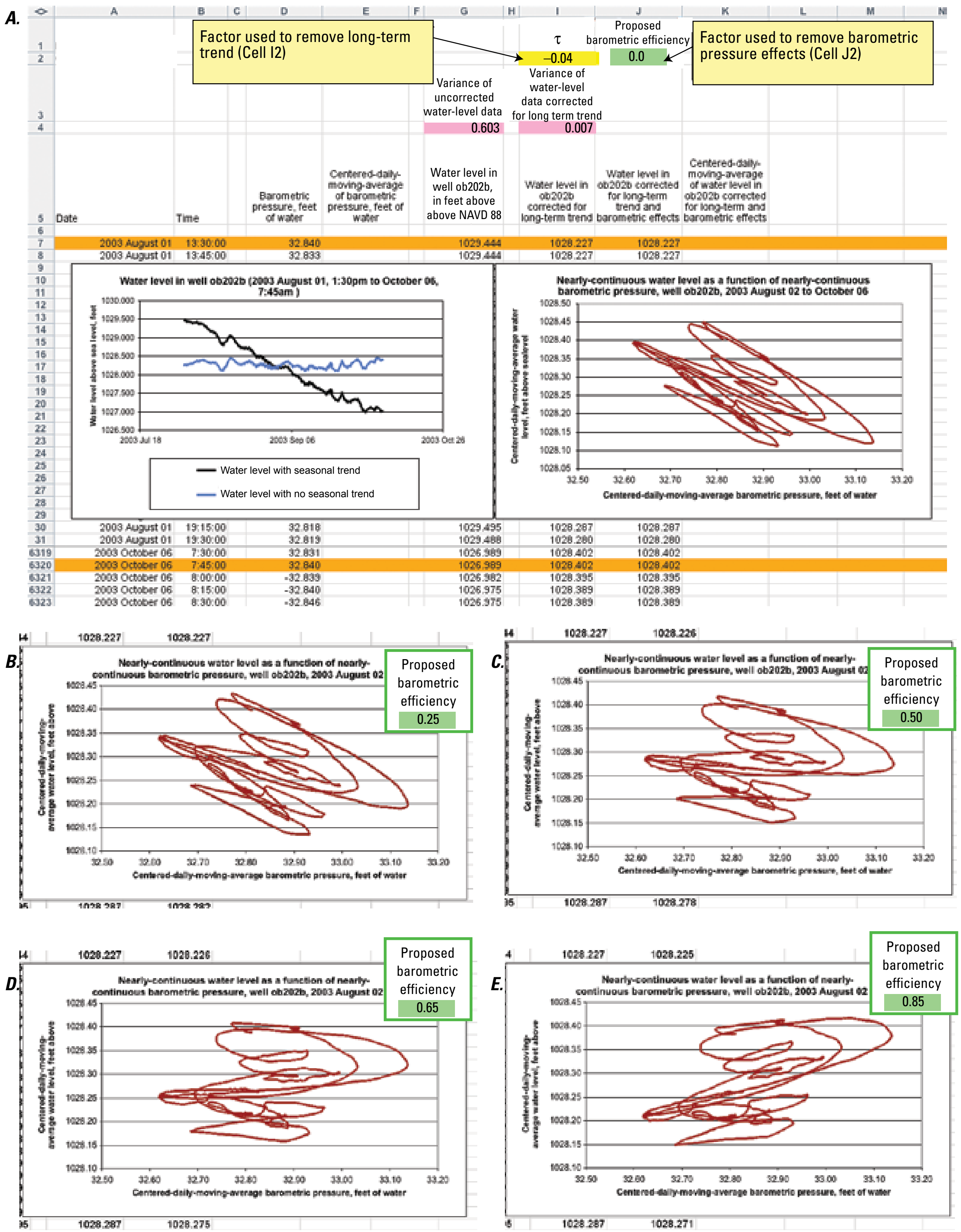

Figure 11. Screen captures of software display showing *(A)* spreadsheet and selected proposed barometric efficiency (BE) values. The spreadsheet is used to estimate the BE by using a proposed BE (a correction factor) to zero the slope of the preferred orientation of the loops on the graph. BE = 0.0 (shown in green). Selected proposed BE values (shown in green) are *(B)* 0.25, *(C)* 0.50, *(D)* 0.65, and *(E)* 0.85.

Increasing the correction factor *m* from zero will increase the slope of the preferred orientation of the elliptical loops on the graph. Figure 11*B* shows that a proposed barometric efficiency of 0.25, assigned to cell J2, increases the slope of the preferred orientation of the loops (fig. 11*B*) compared to a proposed barometric efficiency of zero (fig. 11*A*). Figure 11*C* shows that a proposed barometric efficiency of 0.50 makes the slope of the preferred orientation closer to horizontal. At the point that the correction factor *m* creates a preferred orientation on the graph that is horizontal (fig. 11*D*, proposed barometric efficiency of 0.65, slope is near zero), the proposed barometric efficiency will be the estimate of barometric efficiency of the well for that period of record. Further increasing the correction factor *m* would create a preferred orientation with a *positive* slope (fig. 11*E*, proposed barometric efficiency of 0.85), indicating that the proposed barometric efficiency is greater than the actual barometric efficiency.

Application to a Site in the Piedmont Province, Air Force Plant 6, Marietta, Georgia

The Air Force Plant 6 study site is located on about 150 acres in northern Georgia in the Piedmont Province (fig. 1), which is underlain by fractured-crystalline metamorphic rock with igneous intrusions. The crystalline rock yields limited amounts of water, except where fractures connect to surface water. The rock is weathered toward the surface and is covered by a regolith of saprolitic material referred to as the overburden. A transition zone of intermediate weathering lies between the crystalline rock and the overburden. Some monitor wells are screened in the overburden and transition zone. Most monitor wells are open to the fractured-crystalline rock. Deeper wells open to the fractured-crystalline rock are under more confined conditions than wells screened in the overburden. Wells open to the fractured-crystalline rock have higher barometric efficiencies than wells screened in the overburden.

The aquifer test that was conducted during August and September 2003 occurred as three steps of constant discharge. The total pump duration lasted 889 hours (37 days). The aquifer test was performed in fractured-crystalline rock. During the test, pressure transducers monitored water levels in 45 wells and a retention pond. Two barometers also monitored barometric pressure. The frequency of record was once every 15 minutes. Monitoring continued months after the end of the aquifer test. Beginning about 2 days after the start of the test, barometric pressure rose and fell during a period of about 5 days by a maximum pressure of 10 millimeters of mercury (mm of Hg) (equivalent to about 0.43 foot of water). Several wells responded with a water-level decline followed by a water-level increase. The barometric effects on water level had to be removed to better interpret the aquifer-test data.

The graphical method was used to assess which wells had water levels affected by barometric-pressure changes during the constant-discharge aquifer test and to estimate barometric efficiency. The centered daily-moving average of water level was plotted as a function of centered daily-moving-average barometric pressure. Long-term, barometric-pressure-independent water-level change was removed from the data by using equations 28 and 29. The plots of water level as a function of barometric pressure from wells contained elliptical loops with an observable slope of preferred orientation (see figs. 7–10 for examples). Slopes of the preferred orientation were determined using the two previously mentioned techniques. The negative of the slopes yielded estimates of barometric efficiency.

Barometric-efficiency estimates of the graphical method are listed in table 2 with those of other methods. Barometric-efficiency estimates from the graphical method, using both techniques, ranged from –0.138 to 0.703. The graphical method provided a rapid assessment of whether a well was affected by barometric-pressure change and also provided a rapid estimate of barometric efficiency. Using a correction factor to make the slope of the preferred orientation of the elliptical loops equal zero (technique 2, previously discussed) provided more consistent and reproducible results than the direct measurements of the preferred orientation of the elliptical loops (technique 1).

For a given data set, a wide range of proposed barometric efficiencies should be used with technique 2 in order to identify the slope of the preferred orientation of the loops. In some cases, a broad range (for example, from –3 to 3) will help. Unlike the other methods that are reported to three decimal places, technique 2 of the graphical method is reported to only two decimal places.

Comparison of Methods

This section compares the graphical method with four other methods. The performance of the methods were assessed in two ways: (1) the number of estimates that were outside the domain of the barometric efficiency (less than zero or greater than one), and (2) the results from six control wells where barometric efficiency is determined to be zero based on a strong surface influence on water levels. The two barometric-efficiency methods that used the median values of water-level change divided by barometric-pressure change appeared to be most resistant to barometric-pressure-independent water-level change. Details are discussed below.

Barometric efficiencies were estimated for 45 wells at Air Force Plant 6 using a total of eight versions of five methods (table 2). Two data sets were used for the Clark method: (1) 15-minute data and (2) inflection-centered time intervals. The ordinary-least-squares method was used on both water level and barometric pressure, and water-level change and barometric-pressure change. Study periods were from August through October 2003 for wells that did not respond to the constant-discharge aquifer test. Study periods were from October to December 2003 for wells that did appear to respond to the constant-discharge aquifer test. Up to 20 time intervals

Table 2. Barometric efficiencies of wells using the average-of-ratios, median-of-ratios, Clark, slope, and graphical methods, Air Force Plant 6, Marietta, Georgia, 2003.

[*n*, number of time intervals for methods that used the inflection-centered selection technique; inflection-centered selection technique, time intervals were selected during times when barometric-pressure change was most rapid; OLS, ordinary least squares water level plotted on the y-axis and barometric pressure plotted on the x-axis; OLS Δ, ordinary least squares with water-level change (ΔW) plotted on the y-axis and barometric-pressure change (ΔB) plotted on the x-axis; Technique 1, directly fitting a line to the preferred orientation of the major axes of the elliptical loops; Technique 2, using a correction factor to make the slope of the preferred orientation of the major axes of the elliptical loops be zero. Shading is for wells that are determined to have a barometric efficiency that is near zero based on surface influences on water levels. Theoretically, barometric efficiency should be between zero and one]

Well name	*n*	Average of ratios	Median of ratios	Clark[1]		Slope[2]		Graphical		Standard deviation of all methods
						OLS Δ	OLS			
		Inflection-centered selection technique		All 15-minute increments	Inflection-centered selection technique	Inflection-centered selection technique		Tech-nique 1	Tech-nique 2	
b4mwh	20	0.236	0.270	0.263	0.230	0.222	0.219	0.353	0.29	0.045
b4mwi	20	0.265	0.277	0.287	0.259	0.256	0.254	0.436	0.29	0.060
b4mwq	19	0.532	0.551	0.501	0.494	0.446	0.435	0.555	0.52	0.045
mw-00-102a	20	0.056	0.065	–0.005	0.032	0.006	0.163	0.000	0.00	0.057
mw-00-102b	20	–0.046	0.004	–0.008	–0.066	–0.087	0.097	0.000	0.00	0.056
mwg05	20	0.357	0.350	0.368	0.348	0.335	0.264	0.379	0.36	0.035
mwg10	20	0.364	0.350	0.370	0.354	0.341	0.274	0.387	0.37	0.034
mwg11	20	–0.156	–0.040	–0.093	–0.203	–0.230	–0.030	0.027	0.06	0.106
mwg21	20	0.123	0.128	0.141	0.138	0.153	0.182	0.169	0.14	0.020
mwg5-5r	20	0.541	0.571	0.538	0.524	0.492	0.369	0.584	0.50	0.067
mwos01	20	0.112	0.164	0.143	0.104	0.083	0.036	0.134	0.12	0.039
mwos02	12	0.192	0.128	0.132	0.174	0.160	0.226	0.162	0.13	0.034
mwos03	20	–0.025	–0.055	0.010	–0.018	–0.020	–0.103	0.076	0.07	0.060
mwos04	20	–1.270	–0.352	–0.769	–0.930	–0.677	–0.877	–0.045	0.00	0.447
mwos09	20	0.108	0.012	0.094	0.050	0.004	0.185	0.049	0.04	0.059
mwos10	20	0.068	0.028	0.059	0.032	0.003	0.168	0.021	0.01	0.053
mwos11	20	0.080	0.021	0.087	0.048	0.025	0.071	0.060	0.07	0.025
mwos12	20	0.089	0.035	0.094	0.050	0.020	0.132	0.070	0.05	0.036
mw-w2	20	0.541	0.502	0.503	0.493	0.458	0.392	0.522	0.48	0.046
ob202a	20	0.122	0.014	0.046	0.038	0.013	–0.080	0.000	0.00	0.056
ob202b	20	0.698	0.727	0.677	0.662	0.627	0.453	0.703	0.65	0.086
ob203a	12	0.408	0.391	0.362	0.386	0.370	0.346	0.458	0.39	0.034
ob203b	12	0.401	0.381	0.341	0.377	0.363	0.332	0.425	0.34	0.033
ob203c	20	–0.894	–0.566	–0.682	–0.992	–1.003	1.565	–0.138	–0.13	0.850
ob204b	20	0.051	0.215	0.146	0.046	0.046	0.038	0.341	0.28	0.119
ob204c	20	0.019	0.211	0.111	0.019	0.019	–0.049	0.257	0.26	0.122
ob205a	20	–0.021	0.213	0.078	–0.040	–0.050	–0.282	0.212	0.25	0.180
ob205b	20	0.043	0.043	0.055	0.050	0.058	0.059	0.063	0.05	0.007
ob208a	20	0.327	0.317	0.335	0.299	0.269	0.205	0.393	0.28	0.055
ob208b	18	0.244	0.202	0.247	0.206	0.172	0.170	0.288	0.25	0.042
ob208c	20	0.179	0.133	0.165	0.140	0.104	0.124	0.162	0.17	0.026
ob209a	20	0.030	0.177	0.112	0.024	0.020	–0.002	0.284	0.19	0.104
pmw7d	20	0.279	0.269	0.272	0.270	0.265	0.239	0.272	0.27	0.012
rw201	20	0.147	0.151	0.096	0.084	0.041	–0.047	0.101	0.09	0.063
rw202	20	0.705	0.749	0.686	0.668	0.634	0.452	0.687	0.67	0.089
rw203	12	0.412	0.378	0.323	0.379	0.360	0.309	0.443	0.42	0.047
rw204	20	–0.136	–0.024	–0.055	–0.113	–0.074	–0.008	0.007	0.00	0.054
rw205	20	–0.834	0.071	–0.127	–0.429	–0.218	–0.064	0.134	0.16	0.334
rw207	20	–1.012	–0.721	–0.879	–1.103	–1.083	–0.599	0.013	0.00	0.454
sct1	19	–0.053	0.040	–0.040	–0.100	–0.150	0.259	0.013	0.00	0.123
sct3	20	0.120	0.136	0.187	0.112	0.070	0.442	0.076	0.09	0.122
sct4	20	0.069	0.068	0.097	0.051	0.024	0.162	0.070	0.04	0.042
sct5	20	–0.116	–0.046	0.004	–0.193	–0.212	0.119	0.020	0.04	0.117
sct6	20	0.210	0.197	0.194	0.166	0.141	0.121	0.256	0.14	0.045
sct7	20	0.033	0.037	0.046	0.019	0.006	0.018	0.066	0.05	0.020

[1]Clark, 1967

[2]Ferris and others, 1962

were selected about inflection points of barometric-pressure fluctuations for use in the average-of-ratios, median-of-ratios, Clark, and slope methods. The sample size used for ordinary least squares on water level and barometric pressure was twice that used for other methods using values from both the beginning and end of each time interval.

A total of 360 estimates of barometric efficiency are listed in table 2. Values ranged from –1.270 to 1.565. Results indicate that method consistency varied by well. The standard deviations of method estimates by well ranged from 0.007 to 0.850.

Barometric-Efficiency Estimates Compared to the Domain of the Barometric Efficiency

Method performance was partly assessed by the relative number of barometric-efficiency estimates that were less than zero or greater than one, outside the domain of the barometric efficiency. While estimates that are between zero and one are not necessarily correct, estimates of less than zero or greater than one are known to be incorrect. Table 3 lists the number of estimates that were less than zero or greater than one, which was about 18 percent (64) of all estimates. The methods with the least number of estimates outside the domain of the barometric efficiency were the two techniques of the graphical method followed by the median-of-ratios method. The Clark method using 15-minute data had fewer estimates outside of the domain than the Clark method using the data from 20 inflection-centered time intervals.

Barometric-Efficiency Estimates of Control Wells

Six of the 45 wells were determined to have barometric efficiencies close to zero based on strong surface influences on water levels. Table 4 lists the depths to the tops and bottoms of well openings and justification for determining whether the well has a barometric efficiency near zero (surface influence). There are two lines of evidence that can potentially indicate that a well is not affected by barometric-pressure changes: (1) top of screen is above the water table and (2) well opening is connected to a surface-

Table 3. Number of estimates, by method, that were outside the domain of the barometric efficiency for 45 wells at Air Force Plant 6, Marietta, Georgia, 2003.

[>, greater than; <, less than; –, negative; 15-minute, all 15-minute increments were used; OLS, ordinary least squares best-fit technique was used on the slope method[2]. Inflection centered, time intervals were selected about inflection points of barometric-pressure fluctuations; ΔW, water-level change on the y-axis; ΔB, barometric-pressure change on the x-axis; W, water level on the y-axis; B, barometric pressure on the x-axis; technique 1, direct measure of the slope of the preferred orientation of elliptical loops; technique 2, use of a proposed barometric efficiency to make the slope of the preferred orientation of elliptical loops be zero]

Method name	Type of data	Number of barometric-efficiency estimates				
		>1	<0	<–0.05	<–0.10	<–0.50
Average of ratios	Inflection centered	0	11	8	7	4
Median of ratios	Inflection centered	0	7	4	3	2
Clark[1]	15-minute	0	9	6	4	3
Clark[1]	Inflection centered	0	11	9	7	3
Slope[2], OLS on ΔW and ΔB	Inflection centered	0	11	9	7	3
Slope, OLS on ΔW and ΔB	Inflection centered	1	11	6	4	2
Graphical method—Technique 1	15-minute	0	2	1	1	0
Graphical method—Technique 2	15-minute	0	1	1	1	0
Total		**1**	**63**	**44**	**34**	**17**

[1]Clark, 1967

[2]Ferris and others, 1962

water feature. Control need not be limited to wells. The water levels in the retention pond or any other 15-minute data set not correlated to barometric pressure could have been used as a control.

Water levels in the six control wells do not appear to respond to barometric-pressure change. Instead the wells respond to surface influences such as water-level fluctuations in a retention pond, evapotranspiration, or rain events. The top of the well screen for mwos04 usually is above the water table; thus, this well is not influenced by barometric effects. While a barometric-pressure change may take time to migrate through the unsaturated zone, the pressure may be able to translate to the well quickly when the well is directly connected to surface water. Wells rw207 and ob203c were connected to a nearby retention pond. Water levels in these two wells closely followed those in the retention pond (fig. 12). Surface-water fluctuations in the pond were caused by storm runoff and a pump station. During the growing season, water levels in wells mwg11 and mwos10 declined during daylight hours and rebounded during the night indicating evapotranspiration effects. Because evapotranspiration occurs close to the surface, it is assumed that these two wells are directly connected to soil moisture and were not affected by barometric-pressure fluctuations. Wells mwos10 and sct5 appeared to be responding to nearby Rottenwood Creek; however, no stage data were collected at the site.

Table 4. Control wells with barometric efficiencies determined to be zero based on surface influences, Air Force Plant 6, Marietta, Georgia, 2003.

[TZ, transition zone, partially weathered bedrock; overburden, fully weathered bedrock and fill]

Well name	Top of opening (feet below land surface)	Bottom of opening (feet below land surface)	Hydrogeologic unit	Surface influence
mwos04	13	23	Overburden	Top of well screen is above the water table.
rw207	85	200	TZ	Directly connected to a retention pond.
ob203c	24.2	29.2	Overburden	Very shallow, connected to a retention pond.
mwg11	65	95	TZ	Evapotranspiration dominates water levels during the growing season.
mwos10	66.5	97	Bedrock	Evapotranspiration dominates water levels during the growing season; might be connected to stream.
sct5	57	77	Overburden	Unconfined response to rain events; might be connected to stream.

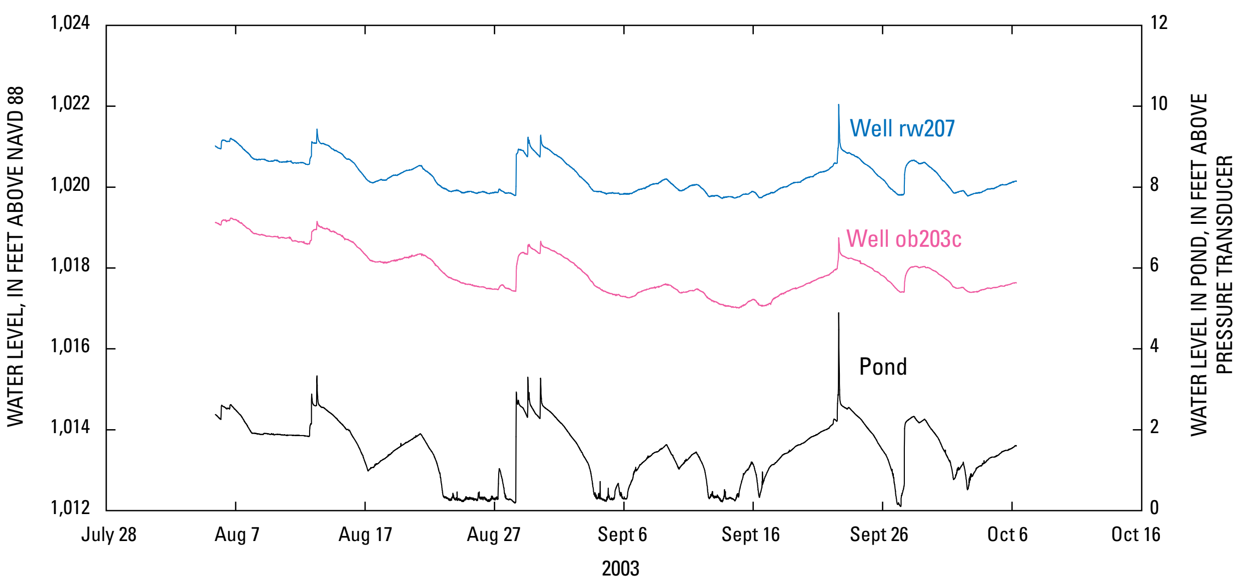

Figure 12. Water levels in wells rw207 and ob203c, and in a nearby pond, Air Force Plant 6, Marietta, Georgia, 2003. See figure 1 for well and pond locations.

Estimates of barometric efficiency for the six control wells are summarized in table 5. Estimates for all methods ranged from –1.270 to 0.068. Excluded from table 5 are results of the Clark method using the inflection-centered time intervals, technique 1 of the graphical method, and the ordinary least squares of water level as a function of barometric pressure. Table 5 also lists variances of ΔW and ΔB for the 19–20 time intervals that were used in the average-of-ratios, median-of-ratios, and slope methods.

The two methods that used the median values of $\Delta W/\Delta B$ or $\overline{\overline{\Delta W}}/\overline{\overline{\Delta B}}$ from time intervals or barometric-pressure fluctuations, respectively, appeared to be most resistant to barometric-pressure-independent water-level change. The graphical method was particularly resistant to large amounts of barometric-pressure-independent water-level change. Because barometric efficiencies for the six control wells are assumed to be zero, the barometric efficiency estimate of a given method is equivalent to the error in the barometric efficiency estimate for that method. The closer an estimate is to zero, the smaller is the error. The error of each method was determined from the average and standard deviation of the barometric efficiencies of the six control wells. The method with the smallest average and standard deviation was the graphical method (–0.003 and 0.067, respectively) followed by the median-of-ratios method (–0.283 and 0.313, respectively).

If barometric efficiencies for all of the wells are zero, the variance of ΔW is equivalent to the variance of ΔW_i. The ratio of the variance of ΔW_i divided by the variance of ΔB appears to be a predictor of the amount of error that might occur in the estimates (see example in fig. 13). The wells with the highest ratio of the variance of ΔW_i divided by the variance of ΔB (wells rw207, ob203c, and mwos04) had the largest average error (–0.739, –0.655, and –0.614, respectively). The plots of wells rw207, ob203c, and mwos04 were particularly difficult to objectively determine barometric efficiency using the graphical method.

Table 5. Estimates of barometric efficiency from different methods for wells determined to have barometric efficiencies of near zero based on surface influences, Air Force Plant 6, Marietta, Georgia, 2003.

[*n*, sample size or number of time intervals used for the slope[2], average-of-ratios, and median-of-ratios methods; ΔB, the barometric-pressure change during a time interval; ΔW, water-level change in a well during a time interval. With the barometric efficiencies of the wells determined to be zero, ΔW is equivalent to ΔW_i, the barometric-pressure-independent water-level change; *VW/VB*, the ratio of the variance of ΔW to the variance of ΔB for *n* number of time intervals; OLS, ordinary least squares water level plotted on the y-axis and barometric pressure plotted on the x-axis; average, the average estimate of barometric efficiency of a method for the six control wells; standard deviation of the estimate of barometric efficiency of a method for six control wells; 15-minute increments were used for the Clark[1] method; –, negative]

Well name	*n*	Variance of ΔB (*VB*, in feet)	Variance of ΔW (*VW*, in feet)	*VW/VB*	Barometric-efficiency estimates					
					Average of ratios	Median of ratios	Clark[1]	Slope[2] (OLS)	Graphical	Average barometric-efficiency estimate, by well
mwg11	20	0.030	0.011	0.383	–0.156	–0.040	–0.093	–0.230	0.06	–0.092
mwos04	20	0.030	0.098	3.276	–1.270	–0.352	–0.769	–0.677	0.00	–0.614
mwos10	20	0.030	0.003	0.092	0.068	0.028	0.059	0.003	0.01	0.034
ob203c	19	0.031	0.113	3.636	–0.894	–0.566	–0.682	–1.003	–0.13	–0.655
rw207	20	0.030	0.137	4.459	–1.012	–0.721	–0.879	–1.083	0.00	–0.739
sct5	20	0.030	0.049	1.631	–0.116	–0.046	0.004	–0.212	0.04	–0.066
Average					**–0.563**	**–0.283**	**–0.393**	**–0.534**	**–0.003**	
Standard deviation					**0.561**	**0.313**	**0.427**	**0.453**	**0.067**	

[1]Clark, 1967

[2]Ferris and others, 1962,

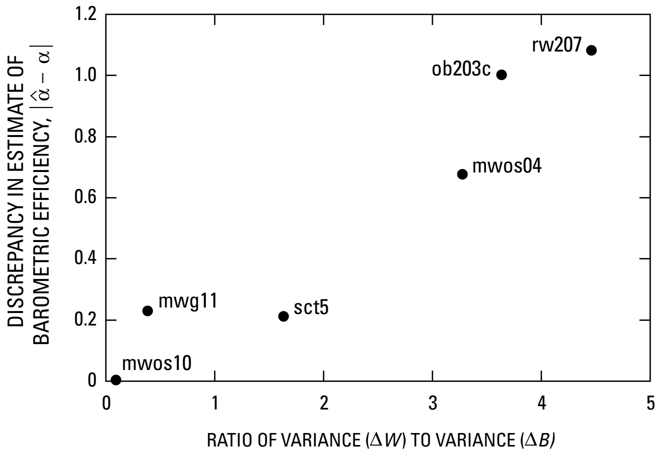

Figure 13. The discrepancy in the estimate of the barometric efficiency as a function of the ratio of the variance of ΔW to the variance of ΔB. The discrepancy is the absolute value of the difference between the actual barometric efficiency (α, determined to be zero) and the estimate of the barometric efficiency ($\hat{\alpha}$) using the slope method (the ordinary least squares best-fit to the slope of ΔW as a function of ΔB). Nineteen to 20 time intervals (19 to 20 values of ΔW and corresponding ΔB) were used. See figure 1 for well locations.

For non-control wells, the variance in values of the ratio of ΔW to ΔB can be used to determine about how much error might occur in the methods. The larger the variance of ratios, the more probable the error will be significant. The variability in the slopes of the loops can be used to determine how much error might occur in the graphical method. The r-squared for the ordinary least squares can be used to determine the probable error in estimations from the slope method.

In the case of a large amount of ΔW_i, many measures of ΔW and ΔB will be required in order to obtain a reliable estimate of barometric efficiency. Methods that use multiple values of ΔW and ΔB to estimate barometric efficiency are superior to the method that estimates barometric efficiency from a single ratio ($\Delta W/\Delta B$). Still, table 5 demonstrates that large amounts of ΔW_i within the study period can cause large errors for most methods. Surface influences on water levels in the control wells created a large amount of ΔW_i.

Water levels in wells ob203c and rw207 correlated to surface-water fluctuations from the retention pond, as can be seen in figure 12 when peaks and troughs coincided with time. Water levels for wells ob203c and rw207 were then corrected for barometric-pressure-independent water-level change in the form of surface-water fluctuations (ΔW_s) using a modified Taylor series:

$$W_{(t)corr} = W_{(t)uncorr} - \sum_{j=1}^{6} a_j \left(S_{(t)} - c_j\right)^j , \qquad (36)$$

where

$W_{(t)corr}$ is the water level corrected for surface-water fluctuations of the retention pond at time t;

$W_{(t)uncorr}$ is the water level not corrected for surface-water fluctuations, at time t;

$S_{(t)}$ is the surface water in the retention pond, at time t;

and

a_j and c_j for wells rw207 and ob203c are listed in table 6.

Values of a_j and c_j were determined in a manner similar to technique 2 of the graphical method (see example in fig. 14). Removing the effects of surface-water fluctuations removed more than 95 percent of the water-level variance for the two wells (table 7).

Table 7 compares the estimates of barometric efficiency for wells rw207 and ob203c before and after surface-water fluctuations were removed from the data. Removing the surface-water fluctuations greatly reduced the ratio of the variance of ΔW_i to the variance of ΔB and greatly reduced the error of most methods. Error reduction usually was more than an order of magnitude. Only the graphical method had a slight increase in the error after the data were corrected for surface-water fluctuations due to the resulting greater precision in the graphical method. The reader is reminded that another set of wells or the same wells but with different study periods will yield slightly different results.

Table 6. Values used to correct wells rw207 and ob203c for barometric-pressure-independent water-level change in the form of surface-water fluctuations from a nearby retention pond, Air Force Plant 6, Marietta, Georgia, 2003. See figure 1 for well locations.

[NA, not applicable; variables are located in equation 36]

rw207				ob203c			
a_j value		c_j value		a_j value		c_j value	
a_1	0.6	c_1	2	a_1	0.495	c_1	2
a_2	0.01	c_2	2	a_2	–0.04	c_2	2
a_3	–0.05	c_3	2	a_3	–0.05	c_3	2
a_4	0.0067	c_4	1.65	a_4	0.0067	c_4	1.65
a_5	0	c_5	NA	a_5	0	c_5	NA
a_6	0.0003	c_6	2.02	a_6	0.0003	c_6	2.02

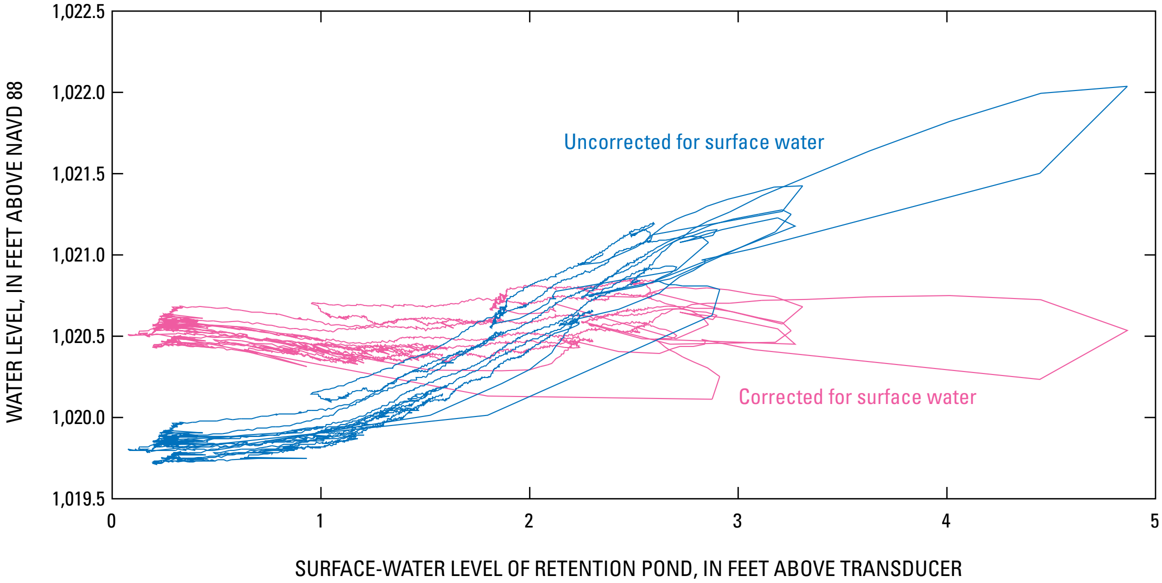

Figure 14. Water level in well rw207 as a function of surface-water level in a nearby retention pond, Air Force Plant 6, Marietta, Georgia, August 5–October 6, 2003. See figure 1 for well location.

Table 7. Estimates of barometric efficiency from different methods for wells ob203c and rw207 before and after water levels were corrected for surface-water fluctuations in a nearby retention pond, Air Force Plant 6, Marietta, Georgia, 2003.

[*n*, sample size or number of time intervals used for the slope[2], average-of-ratios, and median-of-ratios methods; ΔB, the barometric-pressure change during a time interval; ΔW, water-level change in a well during a time interval. With the barometric efficiencies of the wells determined to be zero, ΔW is equivalent to ΔW_i, the barometric-pressure-independent water-level change; *VW/VB*, the ratio of the variance of ΔW to the variance of ΔB for *n* number of time intervals; OLS, ordinary least squares water level plotted on the y-axis and barometric pressure plotted on the x-axis; *uncorr*, uncorrected water-level data; *corr*, water-level data were corrected for surface-water fluctuations in a nearby retention pond; 15-minute increments were used for the Clark[1] method; –, negative]

Well name	*n*	Variance of ΔB (*VB*, in feet)	Variance of ΔW (*VW*, in feet)	*VW/VB*	Barometric-efficiency estimates: Average of ratios	Median of ratios	Clark[1]	Slope[2] (OLS)	Graphical	Average barometric-efficiency estimate, by well
ob203c *uncorr*	19	0.031	0.113	3.636	–0.894	–0.566	–0.682	–1.003	–0.13	–0.655
ob203c *corr*	19	0.031	0.005	0.151	0.084	–0.050	0.132	–0.064	0.06	0.032
rw207 *uncorr*	20	0.030	0.137	4.459	–1.012	–0.721	–0.879	–1.083	0.00	–0.739
rw207 *corr*	19	0.031	0.001	0.040	0.032	–0.020	–0.006	–0.049	–0.02	–0.013

[1]Clark, 1967

[2]Ferris and others, 1962

Summary

Barometric efficiency is the water-level change caused by a barometric-pressure change divided by that barometric-pressure change. Water-level change that is caused by barometric-pressure change cannot be directly measured. The measurable water-level change in a well can be separated into two components: water-level change caused by barometric-pressure change and water-level change not caused by barometric-pressure change, hereinafter referred to as “barometric-pressure-independent water-level change.”

The source of error in the estimate of barometric efficiency is the barometric-pressure-independent water-level change. The key to accurate estimation of barometric efficiency is to reduce the error-causing effect of barometric-pressure-independent water-level changes from the estimation. Some barometric-pressure-independent water-level change can be removed prior to estimating barometric efficiency because it can be identified and avoided or quantified and removed. After avoiding or removing as much barometric-pressure-independent water-level change as possible, some barometric-pressure-independent water-level change will remain in the data.

Methods that estimate barometric efficiency do so in the presence of remaining barometric-pressure-independent water-level change. The best methods for estimating barometric efficiency use many measurements of water-level change and corresponding barometric-pressure change from many time intervals and rely on barometric-pressure-independent water-level change to not be correlated with barometric-pressure change. With many measurements of water-level and barometric-pressure change, the constant relation between the water-level change that is caused by the barometric-pressure change and the barometric-pressure change becomes more apparent while the lack of correlation between the barometric-pressure-independent water-level change and the barometric-pressure change becomes less apparent. A correlation between barometric-pressure-independent water-level change and barometric-pressure change will tend to produce a systematic error. A constant barometric-pressure-independent water-level change with time will cause a random error in the estimate of barometric efficiency.

Time intervals used in methods should be selected such that the barometric-pressure-independent water-level change is as small as possible compared to the barometric-pressure change. Focusing time-interval selection about the inflection points of barometric-pressure fluctuations (when barometric-pressure change is the most rapid) will maximize the value of the barometric-pressure change while not maximizing the barometric-pressure-independent water-level change. The result will be that time intervals will have minimum values of error.

A graphical method was developed that uses continuous water-level and barometric-pressure data to estimate barometric efficiency. A plot of nearly continuous water level (on the y-axis) as a function of nearly continuous barometric pressure (on the x-axis) will plot as a line curved into a series of connected elliptical loops. Each loop represents a barometric-pressure change associated with a barometric-pressure fluctuation. The negative of the slope of the major axis of an elliptical loop will be the ratio of water-level change divided by barometric-pressure change, which is the sum of two ratios—the water-level change caused by the barometric-pressure change divided by the barometric-pressure change (the barometric efficiency) and the barometric-pressure-independent water-level change divided by the barometric-pressure change (the error).

The negative of the slope of the preferred orientation of many elliptical loops is an estimate of the barometric efficiency. The slope of the preferred orientation of many elliptical loops is approximately the median slope of the major axes of the elliptical loops. If the barometric-pressure-independent water-level change does not correlate with barometric-pressure change, the probability that the error will be greater than zero will be the same as the probability that it will be less than zero. As a result, the negative of the median of the slope for many loops will be close to the barometric efficiency. Because there is observational error in using the graphical method, it is advisable that more than one person select the slope or that the same person fits the same data several times in order to minimize subjectivity. Also, a long study period should be used (at least 60 days) to ensure that loops that are affected by large amounts of barometric-pressure-independent water-level change do not significantly contribute error to the barometric-efficiency estimate.

Water-level and barometric-pressure data were collected at Air Force Plant 6, Marietta, Georgia, as part of ground-water characterization efforts. The study site is located on about 150 acres in northern Georgia in the Piedmont, which is underlain by fractured-crystalline metamorphic rock with igneous intrusions.

An 889-hour (37-day) constant-discharge aquifer test was conducted in the fractured-crystalline rock during August and September 2003. Pressure transducers installed in more than 45 observation wells and a retention pond monitored water levels during the test. Two barometers also monitored barometric pressure. The frequency of record was once every 15 minutes. Monitoring continued months after the end of the aquifer test. The barometric effects on water level had to be removed to better interpret the aquifer-test data.

The graphical method was used to assess which wells had water levels affected by barometric-pressure changes. Long-term, barometric-pressure-independent water-level change was removed from the data. The centered daily-moving average of water level was plotted as a function of centered daily-moving-average barometric pressure. Barometric-efficiency estimates from the graphical method ranged from –0.138 to 0.703. The graphical method provided a rapid assessment of whether or not a well was affected by barometric-pressure change and also provided a rapid estimate of barometric efficiency. Barometric efficiency was best determined by using a correction factor to zero the slope of the preferred orientation of loops in corrected water-level data as a function of barometric pressure. The correction factor that zeroed the slope of the preferred orientation of the loops was the estimate of the barometric efficiency.

The graphical method was compared to the average-of-ratios, median-of-ratios, Clark, and slope methods. Estimates of barometric efficiency of the four other methods ranged from –1.270 to 1.565. The performance of the methods were assessed in two ways: (1) the number of estimates that were outside the domain of the barometric efficiency (less than zero or greater than one), and (2) the results from six control wells where the barometric efficiency is determined to be near zero based on a strong surface influence on water levels.

The two methods that used the median values of water-level change divided by barometric-pressure change appeared to be most resistant to barometric-pressure-independent water-level change. The graphical method was particularly resistant to large amounts of barometric-pressure-independent water-level change, having an error that was less than the other four methods. The methods with the least number of estimates outside the domain of the barometric efficiency were the graphical method followed by the median-of-ratios method. Six of the 45 wells were determined to have a barometric efficiency near zero based on strong surface influences on water levels. Because the barometric efficiencies for the six control wells are determined to be zero, the barometric efficiency estimate of a given method is equivalent to the error in the barometric efficiency estimate for that method. The methods with the least average and standard deviation (error) for the six control wells were the graphical method (–0.003 and 0.067, respectively) followed by the median-of-ratios method (–0.283 and 0.313, respectively).

For non-control wells, the variance in values of the ratio of ΔW to ΔB can be used to determine about how much error might occur in the methods. The larger the variance of ratios, the more probable the error will be significant. The variability in the slopes of the loops can be used to determine how much error might occur in the graphical method. The r-squared for the ordinary least squares can be used to determine the probable error in estimations from the slope method.

Methods that use multiple values of water-level change and barometric-pressure change to estimate barometric efficiency are superior to the method that estimates barometric efficiency from a single ratio of water-level change to barometric-pressure change. Still, large amounts of barometric-pressure-independent water-level change within the data can cause large errors for most methods. In the case of a large amount of barometric-pressure-independent water-level change, many measures of water-level change and barometric-pressure change will be required to obtain a reliable estimate of barometric efficiency.

Two of the six control wells had a large ratio of the variance of barometric-pressure-independent water-level change to the variance of barometric-pressure change. Estimates from the average-of-ratios, median-of-ratios, Clark, and slope methods for these wells were largely in error. Water levels in these wells were corrected for surface-water fluctuations, thereby reducing the amount of barometric-pressure-independent water-level change. Estimates for these two wells, after surface-water effects were removed, had errors that were usually more than an order of magnitude smaller than estimates from the uncorrected water-level data.

References Cited

Batu, Vedat, 1998, Aquifer hydraulics: A comprehensive guide to hydrogeologic data analysis: New York, N.Y., John Wiley & Sons, Inc., p. 67–78.

Clark, W.E., 1967, Computing the barometric efficiency of a well, *in* Proceedings of the American Society of Civil Engineers: Journal of the Hydraulics Division, v. 93, no. HY 4, p. 93–98.

Crawford, L.A., 1994, Water level and gradient responses to barometric loading at the Savannah River site: University of Georgia, Athens, Georgia. Master of Science thesis, 140 p.

Davis, D.R., and Rasmussen, T.C., 1993, A comparison of linear regression with Clark's method for estimating barometric efficiency of confined aquifers: Water Resources Research, v. 29, no. 6, p. 1849-1854.

Domenico, P.A., 1983, Determination of bulk rock properties from ground-water level fluctuations: Bulletin of the Association of Engineering Geologists, v. 20, no. 3, p. 283–287.

Ferris, J.G., Knowles, D.B., Brown, R.H., and Stallman, R.W., 1962, Theory of aquifer tests: U.S. Geological Survey Water-Supply Paper 1536-E, 174 p.

Freeze, R.A., and Cherry, J.A., 1979, Groundwater: Englewood Cliffs, N.J., Prentice-Hall, Inc., 604 p.

Galloway, D.L., and Rojstaczer, S.A., 1988, Analysis of the frequency response of water levels in wells to earth tides and atmospheric loading, *in* Proceedings of the Fourth Canadian/American Conference on Hydrogeology—Fluid Flow, Heat Transfer and Mass Transport in Fractured Rocks. Banff, Alberta, Canada, June 21–24, 1988: Dublin, Ohio, U.S.A., National Water Well Association, p. 100–113.

Geldon, A.L., Earle, J.D., and Umari, A.M.A., 1997, Determination of barometric efficiency and effective porosity, boreholes UE-25 c#1, UE-25 c#2, and UE-25 c#3, Yucca Mountain, Nye County, Nevada: U.S. Geological Survey Water-Resources Investigations Report 97-4098, 17 p.

Gossard, E.E., and Hooke, W.H., 1975, Waves in the atmosphere, atmospheric infrasound and gravity waves—Their generation and propagation: New York, N.Y., Elsevier Scientific Publishing Company, 456 p.

Halford, K.J, 2006, Documentation of a spreadsheet for time-series analysis and drawdown estimation: U.S. Geological Survey Scientific Investigations Report 2006-5024, 38 p., *http://pubs.usgs.gov/sir/5024*

Hare, P.W., and Morse, R.E., 1999, Monitoring the hydraulic performance of a containment system with significant barometric pressure effects: Ground Water, v. 37, no. 5, p. 755–763.

Jacob, C.E., 1940, On the flow of water in an elastic artesian aquifer: Transactions, American Geophysical Union, v. 21, p. 574–586.

Kruseman, G.P., and de Ridder, N.A., 1991, Analysis and evaluation of pumping test data: The Netherlands, International Institute for Land Reclamation and Improvement, second ed., 377 p.

Landmeyer, J.E., 1996, Aquifer response to record low barometric pressures in Southeastern United States: Ground Water, v. 34, no. 5, p. 917–924.

Marine, I.W., 1975, Water level fluctuations due to earth tides in a well pumping from slightly fractured crystalline rock: Water Resources Research, v. 11, no. 1, p. 165–173.

Ott, Lyman, 1988, An introduction to statistical methods and data analysis: Boston, Mass., PWS-KENT Publishing Company, third ed., 946 p.

Pascal, Blaise, 1973, The physical treatises of Pascal—The equilibrium of liquids and the weight of the mass of the air, Spiers, I.H.B and A.G.H., trans., intro and notes by Frederick Barry: New York, N.Y., Columbia University Press, Records of Civilization No. 28, 181 p.

Rasmussen, T.C., and Crawford, L.A., 1997, Identifying and removing barometric pressure effects in confined and unconfined aquifers: Ground Water, v. 35, no. 3, p. 502–511.

Rinehart, J.S., 1975, Alternations of flow characteristics within geothermal areas by tidal forces: Colorado University, prepared for the National Science Foundation, PB – 247 190, 8 p.

Robinson, E.S., and Bell, R.T., 1971, Tides in confined well-aquifer system: Journal of Geophysical Research, v. 76, no. 8, p. 1857–1869.

Rojstaczer, Stuart, and Agnew, D.C., 1989, The influence of formation material properties on the response of water levels in wells to Earth tides and atmospheric loading: Journal of Geophysical Research, v. 94, no. 12, p. 12403–12411.

Spane, F.A., Jr., 1999, Effects of barometric fluctuations on well water-level measurements and aquifer test data: Prepared for the U.S. Department of Energy under Contract DE-AC06-76RLO 1830, Pacific Northwest National Laboratory, PNNL-13078, 48 p.

Todd, D.K., 1959, Groundwater hydrology: New York, N.Y., John Wiley & Sons, Inc., 535 p.

Toll, J.N., and Rassmussen, T.C., 2007, Removal of barometric pressure effects and earth tides from observed water levels: Ground Water, v. 45, no. 1, p. 101–105.

Weeks, E.P., 1979, Barometric fluctuations in wells tapping deep unconfined aquifers: Water Resources Research, v. 15, no. 5, p. 1167–1176.

Yilmaz, Oz, and Doherty, S.M., eds., 1987, Seismic data processing: Tulsa, Okla., Society of Exploration Geophysicists, 526 p.

Manuscript approved for publication, June 5, 2007
Prepared by USGS Georgia Water Science Center
Edited by Patricia L. Nobles
Graphics by Bonnie J. Turcott
Layout by Caryl J. Wipperfurth

For more information concerning the research in this report, contact
USGS Georgia Water Science Center, Atlanta
telephone: 770-903-9100